Tetraspanin CD37 regulates platelet hyperreactivity and thrombosis

Marcin A. Sowa[1#], Carmen Hannemann[1#], Ivan Pinos Cabezas[1], Elissa Ferreira[1], Bharti Biwas[1], Min Dai[1], Emma M. Corr[1], Macintosh G. Cornwell[1,2], Kamelia Drenkova[1], Angela H. Lee[1], Tanya Spruill[3], Harmony R. Reynolds[4], Judith Hochman[4], Kelly V. Ruggles[2], Robert A. Campbell[5], Coen van Solingen[1], Mark D. Wright[6], Kathryn J. Moore[1], Jeffrey S. Berger[1], Tessa J. Barrett[1*]

Affiliations:
[1]Cardiovascular Research Center, New York University Grossman School of Medicine; New York, NY, USA
[2]Institute for Systems Genetics, New York University Grossman School of Medicine; New York, NY, USA
[3]Department of Population Health, New York University Grossman School of Medicine; New York, NY, USA
[4]Sarah Ross Soter Center for Women's Cardiovascular Research; New York University Grossman School of Medicine, New York, NY, USA
[5]Department of Emergency Medicine, Washington University in St. Louis, St. Louis, MO, USA.
[6]Department of Immunology, Monash University, Melbourne, VIC, Australia

[#]contributed equally
*Corresponding Author: Tessa.Barrett@nyulangone.org

ESC Topic List: Basic Science, Acute Coronary Syndromes

Running title: Tetraspanin CD37 is a Regulator of Platelet Hyperreactivity and Thrombosis

Keywords: Thrombosis, platelets, tetraspanin

ABSTRACT

Aim: To investigate how psychosocial stress contributes to accelerated thrombosis, focusing on platelet activation and hyperreactivity. The specific objective was to identify novel platelet regulators involved in stress-mediated thrombosis, with a particular emphasis on the tetraspanin CD37.

Methods and Results: To explore how stress contributes to platelet hyperreactivity, platelets were isolated from (1) mice that experienced chronic variable stress and stress-free controls (n=8/group) and (2) human subjects with self-reported high and no stress levels (n=18/group), followed by RNA-sequencing. By comparing mutually expressed transcripts, a subset of genes differentially expressed following psychosocial stress was identified in both human and mouse platelets. In both mice and humans, platelet CD37 positively associates with platelet aggregation responses that underlie thrombosis, with *Cd37*$^{-/-}$ platelets exhibiting impaired integrin αIIbβ3 signaling, characterized by reduced platelet fibrinogen spreading and decreased agonist-induced αIIbβ3 activation. Consistent with a role for CD37 in regulating platelet activation responses, chimeric mice that received *Cd37*$^{-/-}$ bone marrow experienced a significantly increased time to vessel occlusion in the carotid artery FeCl3 model compared to mice reconstituted with wild-type bone marrow. CD37 deficiency did not alter hemostasis, as platelet count, coagulation metrics, prothrombin time, and partial thromboplastin time did not differ in *Cd37*$^{-/-}$ mice relative to wild-type mice. Consistent with this, bleeding time did not differ between wild-type and *Cd37*$^{-/-}$ mice following tail tip transection.

Conclusions: This study provides new insights into the platelet-associated mechanisms underlying stress-mediated thrombosis. Identifying CD37 as a novel regulator of platelet activation responses offers potential therapeutic targets for reducing the thrombotic risk associated with psychosocial stress. The findings also contribute to understanding how psychosocial stress accelerates thrombotic events and underscore the importance of platelet activation in this process.

INTRODUCTION

Despite substantial declines in cardiovascular disease morbidity and mortality over the last 70 years, it remains the leading cause of death in the US.[1] Even with aggressive management of traditional risk factors (e.g., hypertension, hyperlipidemia, and diabetes), many patients develop cardiovascular events, including myocardial infarction (MI) and stroke. These observations indicate that nontraditional risk factors underlie sustained cardiovascular risk. One likely candidate is psychosocial stress, which has emerged as a significant risk factor for the development and progression of cardiovascular disease.[2-4] Psychosocial stress is associated with increased concentrations of inflammatory biomarkers and the development of atherosclerosis.[5-7] Further, stress is associated with a 2-fold increased risk of MI,[2] with high levels of stress at the time of an MI, increasing the risk of death within the following 2 years by 40%.[7-9] The INTERHEART study found that psychosocial stress accounted for 30% of the population attributable risk of acute MI, more than hypertension (18%), diabetes (10%), abdominal obesity (20%), and physical activity (12%).[4] With approximately a third of US adults (34%) reporting overwhelming stress levels most days,[10] defining the mechanisms by which psychosocial stress contributes to increased cardiovascular events is necessary to reduce stress-associated cardiovascular morbidity and mortality.

Platelets are key contributors to the progression of cardiovascular disease and the development of cardiovascular events.[11-13] Mental stress increases platelet hyperreactivity [14-16] which may explain, in part, the stress-cardiovascular disease relationship.[17] In fact, several studies have shown that a hyperreactive platelet phenotype is positively associated with perceived psychosocial stress. Acute stress has been shown to increase platelet activation and secretion of proinflammatory mediators,[18] processes that underlie the risk of cardiovascular events. [19, 20] To date, underlying mechanisms that contribute to stress-mediated thrombosis are poorly defined, thus limiting the ability to prevent or optimally manage stress-linked cardiovascular events.

The platelet transcriptome is increasingly used to inform platelet biology discoveries and develop diagnostic and prognostic biomarkers.[21-29] For example, our group has used transcriptomics to identify regulators of platelet activity (e.g., *WDR1*, *ABCC4*, *MRP14*) in a range of pathologies.[22, 24, 30] Herein, we utilized a mouse model of chronic variable stress and human clinical cohorts to investigate the underlying mechanisms contributing to platelet hyperreactivity. By integrating platelet transcriptomic analyses from humans and mice, we

identified the tetraspanin CD37 in high-risk stress as a novel regulator of platelet activation responses. Largely uncharacterized in platelets,[31-33] we demonstrate that CD37 positively associates with platelet aggregation responses that underlie thrombosis, with *Cd37*-deficient platelets exhibiting impaired integrin αIIbβ3 signaling, reduced spreading on fibrinogen and decreased agonist-induced αIIbβ3 activation. Furthermore, the absence of CD37 reduces thrombotic risk without altering hemostasis or bleeding susceptibility. This study provides new insight into a stress-induced mechanism contributing to accelerated thrombotic risk mediated by platelets and provides the first direct evidence for CD37 as a regulator of platelet activation responses and thrombotic risk.

MATERIALS AND METHODS

Human Studies. Studies were conducted in accordance with the policies of the New York University Langone Medical Center Institutional Review Board and conform to the principles outlined in the Declaration of Helsinki. Informed consent was obtained from each subject. Patients with peripheral artery disease (PAD) or myocardial infarction (MI) were recruited into clinical studies (NCT02106429, NCT03022552) investigating platelet activity, thrombosis, and cardiovascular disease.

For the PAD study (NCT02106429), men and women scheduled for lower extremity revascularization were enrolled into the Platelet Activity and Cardiovascular Events (PACE) study. They had blood collected before their revascularization procedure, as described in detail elsewhere.[12, 24] Briefly, subjects >21 years old on aspirin were recruited from New York University Langone Medical Center, Bellevue Hospital, or the Veterans Affairs NY Harbor Healthcare System. Major exclusion criteria were the use of NSAIDs (other than aspirin) in the past week, antithrombotic therapy, or any known hemorrhagic diathesis. All patients had a venous blood collection before undergoing lower extremity revascularization. For the PAD study, perceived stress was assessed at the time of blood collection by a validated stress questionnaire that queried perceived stress at work and home.[2] Perceived stress was defined as feeling irritable, filled with anxiety, or having sleeping difficulties due to conditions at work or home, and responses were graded as 1) never, 2) some periods, 3) several periods, or 4) permanent.

For the MI study (NCT03022552), women referred for invasive coronary angiography with or without acute coronary syndrome were enrolled in the Heart Attack Research Program (HARP)

study. Arterial blood was collected for platelet transcriptome and activity measures at the time of coronary angiography from MI patients and CV controls. A self-report measure was obtained to assess perceived stress (Perceived Stress Scale [PSS-4]), a reliable and valid tool for perceived stress in the past month.[34]

Human Platelet Aggregation. After an initial 2 cc discard, blood was collected into 3.2% sodium citrate tubes and allowed to rest for 10 min before isolation of platelet-rich plasma by centrifugation at 200 g. Platelet aggregation was measured in response to submaximal agonist stimulation with epinephrine (2, 0.4, 0.1 μM) and adenosine diphosphate (ADP; 2, 1, 0.4 μM). Platelet aggregometry was conducted on a Helena AggRAM light transmission aggregometer (Beaumont, TX) based on the method of Born.[35] Epinephrine and ADP were purchased from Helena Laboratories.

Human Platelet Activation Assays. Circulating monocyte-platelet aggregates (MPA) were identified in citrate anticoagulated blood as previously described.[12] Briefly, whole blood was fixed with 1% formaldehyde (Sigma-Aldrich) 15 min post-phlebotomy. Fixed whole blood was stained with 5 μL CD61-FITC (Dako) to identify platelets and 5 μL CD14-APC (BD Biosciences) to identify monocytes. After lysis of red blood cells, monocytes were collected based on side-scatter properties and positive staining for CD14 using an Accuri C6 flow cytometer (BD Biosciences, San Jose, CA). Leukocyte-platelet aggregates were identified as $CD45^+CD61^+$ events, monocyte-platelet aggregates as $CD45^+CD14^+CD61^+$ events, and neutrophil-platelet aggregates as $CD45^+CD14^-CD61^+$ based on size.

Human Platelet Transcriptome. Details on blood collection, platelet RNA extraction, and data processing have been previously described.[22, 30, 36, 37] Briefly, platelets were isolated and purified by incubation with microbeads to deplete leukocytes and red blood cells (EasySep™ Human CD45 Depletion Kit II and EasySep™ RBC Depletion Reagent, STEMCELL Technologies). Isolated platelets were lysed in 500 uL of QIAzol Lysis Reagent (Qiagen) and stored at −80°C. RNA was isolated with Direct-zol RNA microspin columns (Zymo Research), and quality and quantity were determined with a Bioanalyzer 2100 (Agilent Technologies). Sequencing libraries were barcoded and prepared using the Clontech SMART-Seq HT with Nxt HT kit (Takara Bio USA), and libraries were sequenced single end on an Illumina NovaSeq 6000. Samples were analyzed using the Seq-N-Slide pipeline.[38] Reads were aligned to the hg38 genome using STAR[39] v2.6.1 and quantified using featureCounts[40] v1.6.3. Read quality was assessed using

FASTQC[41] v0.11.7. Differential expression analysis was performed via DESeq2 v1.24. Multiple hypothesis correction was done using the Benjamini-Hochberg method. Heatmaps were created using ComplexHeatmap[42, 43] v2.0.0, and all plotting was done using ggplot2[44] v3.2.1. WGCNA[45] was used to collapse the expression of gene sets to single eigengene values.

Megakaryocyte Studies. $CD34^+$ stem cells (Fred Hutch Cancer Center, Seattle) were differentiated to megakaryocytes in StemSpan™ Serum-Free Expansion Medium II (SFEM II, STEMCELL Technologies) supplemented with 50 ng/mL recombinant human thrombopoietin (TPO, R&D Systems), 25 ng/mL recombinant human stem cell factor (SCF, R&D Systems), 100 U/mL penicillin and 100 µg/mL streptomycin (Gibco™). Cultures were passaged into fresh TPO-containing media on days 3, 6, and 9.[37] On day 10, megakaryocytes were purified by positive selection of CD42a expressing cells (Anti-Human CD42a-PE, #558819, BD Biosciences), and isolated with the EasySep™ Release Human PE Positive Selection Kit (#17654, STEMCELL Technologies) and allowed to rest overnight. On day 11, cells were treated with 100 µM aspirin (Cayman Chemical), 5 µM $P2Y_{12}$ inhibitor AZD1283 (Cayman Chemicals), or both drugs simultaneously for 24 hours. PBS or 0.025% DMSO were used as vehicle controls for aspirin and AZD1283/dual antiplatelet therapy, respectively.[46] Following incubation, megakaryocytes were lysed in QIAzol® Lysis Reagent (Qiagen) and stored at -80° C before RNA isolated with Direct-zol RNA microspin columns (Zymo Research). RNA library preparation and sequencing are described above in “Human Platelet Transcriptome.”

Western Blots. Platelet protein was extracted in Tyrode’s buffer containing 1% Triton X-100 and 1% cOmplete protease inhibitor cocktail (Roche), and samples (15 µg/well) were electrophoresed on 10% NuPAGE Bis-Tris gels (ThermoScientific) and transferred to polyvinylidene difluoride membrane at 20 V for 7 min. Membranes were blocked for 1 hour in 5% fat-free milk and incubated with rabbit anti-CD37 (ab315346, Abcam) overnight at 4°C.Proteins were detected by chemiluminescence using goat anti-rabbit HRP-conjugated secondary antibody (Cat. 31460, ThermoScientific) and Pierce ECL Western Blotting substrate (ThermoScientific). As loading control, membrane was incubated with HRP-conjugated anti-GAPDH (HRP-60004, Proteintech) after stripping with Restore Western Blot Stripping Buffer (ThermoScientific) and detected using goat anti-rabbit HRP-conjugated secondary antibody and Pierce ECL Western Blotting substrate. Membrane was scanned using the ChemiDoc MP Imaging System (Bio-Rad).

Immunocytochemistry. Platelets were plated on 1.5 round covers glasses coated with 50 µg/mL Poly-D-Lysine (Gibco). Cells were fixed with 2% paraformaldehyde solution for 15 min at room temperature. Samples were washed and blocked for 1 h at room temperature with 5% bovine serum albumin in PBS, followed by overnight incubation at 4°C with rabbit anti-mouse CD37 primary antibody (#PA5-112376, ThermoFisher) at a 1:100 dilution with blocking buffer. Samples were washed and incubated for 1 h at room temperature with goat anti-rabbit IgG cross-adsorbed secondary antibody conjugated with Alexa Fluor™ 568 at a 1:200 dilution in blocking buffer. Samples were washed, permeabilized for 1 h at room temperature with PBS containing 0.1% Triton X-100, and subsequently incubated with Phalloidin iFluor™ 647 (Cayman Chemical) diluted 1:1,000 in PBS containing 1% bovine serum albumin for 1 h at room temperature. Coverslips were washed and mounted with ProLong™ Diamond Antifade (Thermo Fisher), and platelets were imaged using a Zeiss Elyra7 super-resolution microscope (Carl Zeiss, Jena, Germany) equipped with a plan-apochromat 63x/1.4 oil DIC M27 objective. A SIM² image reconstruction algorithm was applied to the Elyra7 images with Lattice SIM² using the Zen Black software (Carl Zeiss).[47]

Animal Studies. The Institutional Animal Care Use Committee of New York University Medical Center approved all animal experiments, and adhere to NIH Guide for the Care and Use of Laboratory Animals. C57BL/6J mice were from Jackson Laboratories (stock number 000664). *Cd37*$^{-/-}$ and wild-type controls rederived mice at NYU from sperm originating from *Cd37*$^{-/-}$ mice from Dr. Mark Wright (Monash University).[48] All mice were housed in a pathogen-free facility at an ambient temperature of 22–25°C. For the chronic variable stress studies, female C57BL/6J mice at 7-10 weeks of age were exposed to a validated protocol of chronic variable stress for 3 weeks.[49] Mice were randomly allocated to treatment groups. For bone marrow transplantation, 10-week-old male wild-type (C57BL/6) mice were subjected to two doses of 4.5 Gy separated by a 4 h interval of total body irradiation followed by reconstitution with 4×10^6 bone marrow cells from wild-type or *Cd37*$^{-/-}$ donor mice via retro-orbital injection. Animals were allowed to recover for 6 weeks after bone marrow transplantation. Experimental procedures were done in accordance with the US Department of Agriculture Animal Welfare Act and the US Public Health Service Policy on Humane Care and Use of Laboratory Animals and were approved by the New York University School of Medicine's Institutional Animal Care and Use Committee.

Pulmonary Embolism Model. Pulmonary embolism was induced under isoflurane (maintenance dose: 1-3% isoflurane with 0.25-1 L/min oxygen) anesthetized mice by injection into the retro-orbital vein plexus 60 mg/kg epinephrine and 150 mg/kg collagen in phosphate-buffered saline (PBS) in a total volume of 200 µL, as described previously.[50] Time to death was monitored for 45 minutes, following breathing cessation and secondary confirmation via toe pinch, mice were euthanized by cervical dislocation. Immediately post-expiration, the chest cavity was exposed, and the lung was removed, rinsed in PBS, and fixed in 10% formalin. Lungs were then paraffin-embedded, sectioned, and microthrombi quantified by CD42b staining (ab227669, Abcam).

$FeCl_3$ Thrombosis. Mice were anesthetized with ketamine (100 mg/kg) and xylazine (10 mg/kg), fur on the neck and upper chest clipped, and mice secured supine. An incision was made on top of the right common carotid artery region; the fascia bluntly dissected, and a segment of the left common carotid artery exposed. Carotid blood flow was measured with a Doppler flow probe MA-0.5PSB (Transonic Systems, Inc., Ithaca, NY) connected to a TS420 perivascular flowmeter module (Transonic Systems, Inc., Ithaca, NY). Thrombosis was induced by applying a 1 x 2mm patch of filter paper soaked in a $FeCl_3$ (5% solution) to the ventral surface of the left carotid artery for 30 seconds.[51, 52] Blood flow was monitored upon removal of the $FeCl_3$-soaked filter paper until flow was completely occluded. Occlusion was defined as blood flow cessation (0 mL/min) for ≥1 min. At the end of the experiment, mice were euthanized by cervical dislocation.

Mouse Platelet Activation Assays. Blood was drawn from isoflurane-anesthetized mice and mixed immediately with heparin. Blood was then diluted in Tyrode's buffer containing 1 mM $CaCl_2$ and 0.35% BSA before stimulation with epinephrine (10 µM, Helena Laboratories), PAR4 AP (50 or 500 µM, Cayman Chemicals), or U46619 (Cayman Chemicals) + adenosine 5′-diphosphate (ADP, 5 µM of each, Helena), in the presence of αIIbβ3 (JON/A-PE; 2 µg/mL, Emfret Analytics) and P-selectin (anti–P-selectin–FITC; 2 µg/mL, Emfret Analytics) antibodies for 15 min to assess platelet activation. Before analysis, samples were diluted in PBS to quench activation and then immediately analyzed on a MACSQuant 16 Flow Cytometer (Miltenyi).
To measure leukocyte-platelet aggregates, retro-orbital drawn blood was immediately fixed and lysed (BD Phosflow) at room temperature for 30 min. After washing, cells were stained with CD45-PerCpCy5.5, Ly6C-BV421, Ly6G-PE, CD11b-APC-Cy7, and CD41-APC at 1:200 for 30 min at 4 ºC, washed and resuspended in FACS buffer before analysis on a MACSQuant 16

Flow Cytometer (Miltenyi) flow cytometer. Leukocyte-platelet aggregates were identified as $CD45^+CD11b^+CD4^+$ events, monocyte-platelet aggregates as $CD45^+CD11b^+Ly6C^+Ly6G^-CD41^+$ events and neutrophil-platelet aggregates as $CD45^+CD11b^+Ly6C^-Ly6G^+CD41^+$ events.

Platelet Spreading Assay. Under isoflurane, mouse blood from the vena cava was collected into 1mL syringes coated with 100 µL citrate-dextrose solution (ACD, Santa Cruz), diluted 1:1 in Tyrode's buffer with 0.3% BSA (Sigma) and centrifuged (20 min, 200 x g, no brake). The platelet-rich plasma (PRP) layer was carefully transferred into a new 5 mL polystyrene tube, and platelets were pelleted (10 min, 1,000 x g, no brake) after adding prostaglandin E1 (PGE1, 1 µM Sigma). The supernatant was discarded, and the pellet was gently resuspended in 500 µL Tyrode's buffer and 1 µM PGE1. The washed platelets were counted, adjusted to a concentration of 1×10^5 platelets/ µL, and let rest for 30 min at RT. To assess platelet spreading dynamics, autoclaved round cover glasses (8 mm, #1.5; Worldwide Medical Products) were coated with either 100 µg/mL filtered fibrinogen (Sigma-Aldrich) in PBS or 50 µg/mL poly-D-lysine (Gibco) diluted in PBS overnight at 4 °C. After removing the coating solution and three washes with molecular grade water (Corning), poly-D-lysine coated cover glasses were dried for two hours under a laminar flow hood. Following three washes with PBS, the fibrinogen-coated cover glasses were blocked with 5 mg/mL heat-denatured BSA (Sigma) in PBS for at least one hour at RT. To poly-D-lysine coated glasses, 150 µL of washed platelets were added. After removing the blocking solution, 100 µL Tyrode's buffer containing 1 µL $CaCl_2$ (1 M) and 50 µL washed platelets were added to the fibrinogen-coated glasses. Platelets adhered for 45 min at 37 °C, fixed in 2% paraformaldehyde solution (Thermo Fisher) for 15 min at RT, and permeabilized in 0.1 % Triton X-100 in PBS for 15 min RT. Following two washes with PBS, actin filaments were stained with Phalloidin iFluor™ 647 (Cayman Chemical) diluted 1:1000 in 0.1 % Triton X-100 in PBS for 1 h at RT, protected from light. After three washes with PBS, cover glasses were mounted with ProLong™ Antifade (Thermo Fisher) and imaged using a 100x objective (and the EdgeStrong image filter) on Keyence BZ-X800. Shape descriptors of single platelets were analyzed using the particle analyzer tool on ImageJ 1.54f. At least 5 images and 650 cells were analyzed per mouse.

Mouse coagulation. Citrated blood was collected by retro-orbital bleed, and 20 uL loaded onto an Element COAG+ test strip and prothrombin time and activated partial thromboplastin time measured on an Element COAG+ analyzer (Heska) according to the manufacturer's instructions.

Bleeding time. Tail bleeding times were measured by clipping 1 mm from the tip of the tail of anesthetized (ketamine and xylazine, 80/12 mg/kg) mice. The tail was placed in prewarmed saline at 37 °C, and the time to bleeding cessation monitored for 10 minutes.

Mouse Platelet Isolation for RNA-Seq. Whole blood was drawn from the vena cava into 10% ACD. Total blood from 2 mice was pooled per sample. Platelets were isolated by centrifugation of whole blood (approx. 2 mL) diluted in Tyrode's buffer (approx. 3mL) at 200 g for 20 min in a swinging bucket centrifuge. Platelet-rich plasma was removed, volume was adjusted to 4 mL with Tyrode's, and PGE1 was added before centrifugation at 1000 g for 10 min to prevent exogenous platelet activation. The platelet pellet was then resuspended in 1800 µL Tyrode's buffer containing 80 µL of anti-Ter-119 microbeads (Miltenyi Biotec) and 80 µL of anti-CD45 microbeads (Miltenyi Biotec), and incubated for 20 min at RT. Samples were passed through MACS LS columns to deplete erythrocytes and leukocytes, fresh PGE1 was added, and collected platelets were centrifuged at 1000 g for 10 min. The platelet pellet was then resuspended in 1mL of Tyrode's, an aliquot was removed for platelet purity assessments, and the remaining platelets were allowed to rest for 15 min. Before centrifugation at 2500 rpm for 10 min, PGE1 was added, and the resulting platelet pellet was resuspended in 600 µL QIAzol® Lysis Reagent (QIAGEN). Total RNA was isolated using Direct-zol RNA MicroPrep columns (Zymo Research).

Statistical Analyses

The statistical significance of differences was evaluated using a two-tailed Student's t test unless otherwise noted. P values of less than 0.05 were considered significant. Normality of data was assessed via a Shapiro-Wilk normality test. Analyses were performed using GraphPad Prism8 (GraphPad Software). Numbers of replicates and statistical tests are indicated in each Figure legend. All data are expressed as mean ± SEM, unless otherwise noted.

RESULTS

Psychosocial Stress Promotes Platelet Hyperreactivity & Thrombosis Susceptibility

To investigate the impact of stress on platelet activity, platelet hyperreactivity biomarkers were analyzed in blood samples of 98 patients with established cardiovascular disease who reported their level of perceived stress (including irritability, anxiety, or sleeping difficulty, **Fig. 1A**, demographics **STable 1**). Blood platelet hyperreactivity biomarkers, leukocyte-platelet aggregates (LPA, $p<0.01$), monocyte-platelet aggregates (MPA, $p<0.05$), and neutrophil-platelet aggregates (NPA, $p<0.05$, **Fig. 1B**) were significantly increased in subjects with higher periods of stress compared to the non-stressed cohort.

To gain insight into the mechanisms by which psychosocial stress promotes platelet hyperreactivity, we examined the impact of stress on platelet phenotype and function in a validated mouse model of chronic variable stress which alternates stressors (e.g., crowding, isolation, cage tilting, light changes) over three weeks (**Fig. 1C**, **SFig. 1A**, **B**).[7] Compared to non–stressed controls, stressed mice had larger (**Fig. 1D**) and more reticulated platelets (**Fig. 1E**), although platelet count did not differ between groups (**SFig. 1C**). Stressed mice had significantly increased circulating levels of the platelet hyperreactivity biomarkers, MPA, proinflammatory Ly6C^{hi}-MPA and NPA relative to stress-free control mice ($p<0.05$, **Fig. 1F**). Furthermore, following ex vivo stimulation with protease-activated receptor 4 activating peptide (PAR4-AP), MPA and NPA formed more readily in stressed mice versus stress-free controls ($p<0.001$, **SFig. 1D, E**). To further study stress-mediated platelet hyperreactivity, platelet surface expression of the activation markers JON/A (activation of integrin αIIbβ3) and P-selectin (alpha granule release) were measured. Platelets from stressed mice were found to be more sensitive to stimulation with epinephrine, PAR4-AP, and combination of thromboxane A2 mimetic (U46619) and adenosine diphosphate (ADP) relative to controls, consistent with stress-mediated platelet hyperreactivity ($p<0.05$, **Fig. 1G**).

To assess whether stress-mediated platelet activity translated to increased thrombotic risk stressed and control mice were injected with collagen and epinephrine, and time to death was monitored.[53] In this model of pulmonary thrombosis, stressed mice demonstrated significantly reduced survival time relative to controls ($p<0.01$, **Fig. 1H, I**) and, at the time of death, had a higher lung-to-body weight ratio (**Fig. 1J**). Moreover, quantification of lung microthrombi revealed increased platelet aggregation in the lungs of stressed mice (**Fig. 1K**). Additionally, stressed mice are more susceptible to arterial thrombosis relative to stress free controls (**SFig.**

1F). These data indicate that stress induces platelet hyperreactivity and accelerates thrombotic risk.

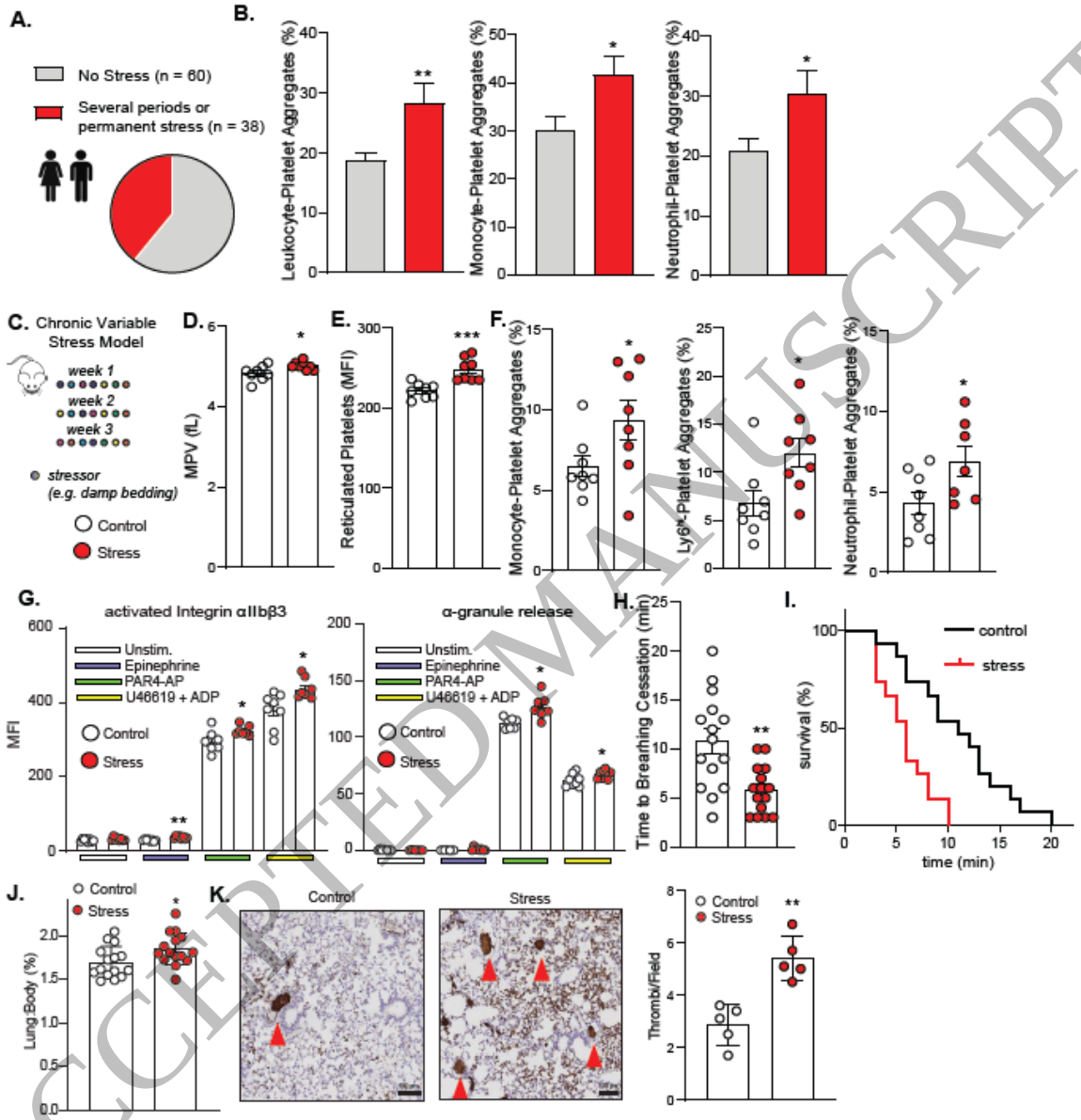

Figure 1. Psychosocial Stress Induces Platelet Hyperactivity and Accelerates Thrombosis

(A) Self-reported stress levels in a cohort of cardiovascular disease patients (n = 98). Circulating blood levels of the stable platelet activation markers **(B)** leukocyte-platelet-aggregates (LPA), monocyte-platelet-aggregates (MPA), and neutrophil-platelet-aggregates (NPA) as measured by flow cytometry at the time of stress questionnaire. Grey bars, no stress (n = 60); red bars, several or permanent periods of stress (n = 38). **(C)** Mouse chronic variable stress model. **(D)** Mean platelet volume (MPV), **(E)** reticulated platelets, and **(F)** quantification of LPA, proinflammatory Ly6C^{hi} MPA, and NPA in stress and control mice. White circles, no stress control mice (n = 8); red circles, stressed mice (n = 8). **(G)** Platelet surface expression of the activation markers activated integrin αIIbβ3 and P-selectin following incubation with PBS

(Unstim.), epinephrine (10 μM), PAR4-activating peptide (PAR4-AP, 500 μM), or U46619 and ADP (5 μM, receptively) for 15 min. White circles, no stress control mice (n = 7-8); red circles, stressed mice (n = 7-8). **(H-K)** Pulmonary embolism was induced in anesthetized mice by retro-orbital injection of 60 mg/kg epinephrine and 150 mg/kg collagen. **(H)** Time to death was monitored for 45 minutes, and **(I)** Kaplan-Meier survival curve. **(J)** Lung-to-body weight ratio at death and **(K)** pulmonary CD42b staining for platelet aggregates and platelet aggregate quantification. White circles; stress-free control mice (n = 15); red circles, stressed mice (n = 15). Scale bar = 100 μM. Mean ± SEM, *p<0.05, **p<0.01, ***p<0.001 by Student's t-test.

CD37 Positively Associates with Aggregation and Regulates Platelet Function

Platelet hyperreactivity constitutes an important thrombotic risk factor, and platelet RNA-sequencing (RNA-seq) can provide unbiased mechanistic insight into platelet activity responses.[22, 24, 37, 54] To investigate platelet-mediated transcripts and pathways regulated by psychosocial stress, platelets were isolated from mice at the end of the three-week stress protocol (n = 8 mice per group) and from human subjects with no versus high levels of reported stress (n = 18 per group, demographics **STable 2**). Transcriptomic analysis by RNA-seq of platelets from stress and no-stress littermate control mice revealed 304 transcripts differentially expressed (140 up, 165 down, p<0.05, **Fig. 2A**, **B**). Within the human cohort, 1394 transcripts were differentially expressed in platelets from moderate to high-stress subjects relative to stress-free participants (537 up, 857 down, p<0.05, **Fig. 2C**, **D**). By comparison of mutually expressed transcripts in our highly purified platelet samples (**SFig. 2A, B**), we identified a subset of genes differentially expressed by psychosocial stress in both human and mouse platelets.

To assess if any of these transcripts were associated with platelet phenotypic responses that contribute to thrombosis, their association with platelet aggregation to epinephrine (0.4 μM), a αIIbβ3-dependent process, was assessed. Platelet *CD37* and *SPPL2B* expression were found to significantly correlate with platelet aggregation responses in a cohort of participants (n = 145) whose platelet aggregation and platelet transcriptome were measured simultaneously (**Fig. 2E**). A larger dynamic range between platelet expression values and aggregation to epinephrine was apparent for CD37 (R = 0.30, p=0.0002, **Fig. 2F**). CD37 is a tetraspanin, a protein class which acts as a molecular scaffold to distribute membrane proteins into organized microdomains for processes including adhesion and signaling.[55] Several tetraspanins have previously been identified as regulators of platelet function[33]; however, the role of platelet CD37 is largely unexplored. In humans, 33 tetraspanins have been identified, 22 of which are present at the transcriptomic level in human platelets (**Fig. 2G**, **STable 3**). Profiling of platelet aggregation responses and correlating with platelet tetraspanin expression reveals that *CD37*, relative to all other platelet tetraspanins, was most associated with platelet aggregation to submaximal

concentrations of epinephrine and ADP (green box, **Fig. 2H**). Of note, psychosocial stress did not alter the expression of leukocyte, monocyte or neutrophil CD37 (**SFig. 2C**-**E**).

By weighted correlation network analysis (WGCNA)[37] the contribution of platelet *CD37* expression to biological pathways associated with platelet activation and aggregation responses was assessed. In a cohort of participants, each sample was assigned an eigengene representing the average gene expression of platelet-associated GO biological pathways, and their association with *CD37* was assessed. This bioinformatics approach revealed that platelet *CD37* expression is positively associated with the gene modules “platelet activation”, “regulation of integrin-mediated signaling pathway”, “platelet aggregation” and “regulation of inflammatory responses to wounding” (**Fig. 2I**-**L**, **STable 4**). Collectively, these data provide evidence that CD37 is a regulator of platelet activation responses.

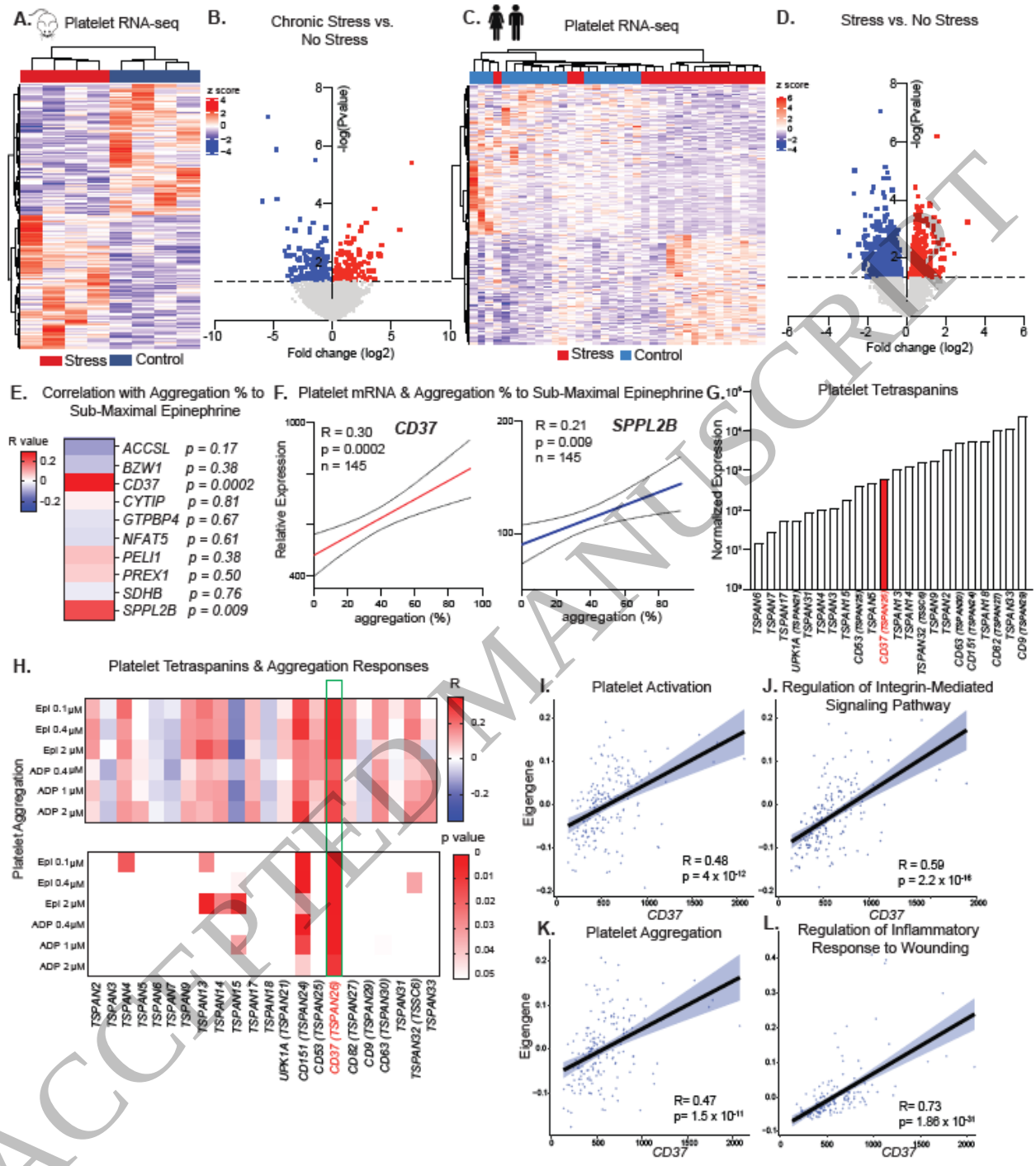

Figure 2. CD37 is Upregulated in Platelets from Stressed Mice and Humans.
Mouse platelet RNA-seq. Platelets were isolated from stress or stress-free control mice at the end of the 3-week chronic variable stress protocol. Platelets were purified, total RNA isolated, and RNA-seq performed. **(A)** Heat map and **(B)** volcano plot of differentially expressed transcripts between stress and control mice ($p<0.01$). n = 4 samples per group, representing blood from 8 pooled mice per phenotype. Platelets isolated from stressed or stress-free control subjects (Demographics **STable 2**, n = 18 subjects per group). Platelets were purified, total RNA isolated, and RNA-seq performed. **(C)** Heat map and **(D)** volcano plot of differentially expressed transcripts between stressed and stress-free control subjects ($p<0.01$). **(E)**

Spearman's correlation of platelet transcript expression versus platelet aggregation responses to 0.4 μM epinephrine (n = 145 subjects). **(F)** Correlation plots of platelet *CD37* and *SPPL2B* relative to aggregation response to 0.4 μM epinephrine (n = 145 subjects). **(G)** Normalized expression levels of the 22 identified human platelet tetraspanins. CD37 is highlighted in red. **(H)** Correlation matrix of platelet tetraspanins and aggregation responses to epinephrine (Epi; 0.1, 0.4 and 2 μM) and adenosine diphosphate (ADP; 0.1, 0.4 and 2 μM) as measured by light transmission aggregometry. Spearmen correlation, R values displayed in the top panel, p-values in the bottom panel. Correlation of platelet *CD37* expression (x-axis) and the relative eigengene values for pathways **(I)** platelet activation, **(J)** integrin-mediated signaling, **(K)** platelet aggregation and **(L)** regulation of inflammatory responses to wounding (y-axis, n = 183). Associations were assessed by Spearman's rank correlation coefficient.

CD37 Deficiency Does Not Alter Hemostasis

CD37 has previously been investigated in various myeloid cells [48, 56-62], however, its contribution to platelet function has not been assessed. We first confirmed the presence of megakaryocyte and platelet CD37 at the transcriptomic (**Fig. 3A**) and protein level (**Fig. 3B**, **C, SFig. 3, SFig. 4**) in wild-type and *Cd37*$^{-/-}$ mice. Relative to wild-type mice, platelet count (**Fig. 3D**), and coagulation metrics, prothrombin time (**Fig. 3E**), and partial thromboplastin time (**Fig. 3F**) do not differ in *Cd37*$^{-/-}$ mice indicative of no differences in hemostatic parameters. Consistent with this, bleeding time does not differ between wild-type and *Cd37*$^{-/-}$ mice following tail tip transection (**Fig. 3G**).

Platelet CD37 Regulates Cytoskeletal-dependent Adhesion and Spreading

Based on the role of other platelet tetraspanins and our data demonstrating a robust link between platelet CD37 and platelet aggregation (**Fig. 2**), we reasoned that CD37 is a regulator of platelet cytoskeletal-dependent processes in part by modulation of integrin αIIbβ3 signaling. To assess the contribution of platelet CD37 to adhesion and spreading, platelets from wild-type and *Cd37*$^{-/-}$ mice were adhered to poly-D-lysine (50 μg/mL) or the αIIbβ3-ligand, fibrinogen (100 μg/mL) for 45 min. *Cd37*$^{-/-}$ platelets plated on both poly-D-lysine (**Fig. 3H**-**J**) and fibrinogen (**Fig. 3K**-**M**) spread significantly less relative to wild-type platelets as noted by increased platelet circularity (**Fig. 3I, L**) and reduced perimeter (**Fig. 3J, M**).

Following adhesion to fibrinogen, platelets become activated and undergo substantial cytoskeletal remodeling, mediated by integrin αIIbβ3, resulting in platelet shape change and spreading.[63] Following adhesion to fibrinogen, *Cd37*$^{-/-}$ platelets underwent a minimal change in morphology, maintaining a round shape and forming a smaller number of filopodia (**Fig. 3N**). Platelet solidity, a proxy measure inversely proportional to efficient maximal spreading mediated by filopodial-to-lamellipodial transitions, was significantly increased in *Cd37*$^{-/-}$ platelets relative

to wild-type (p<0.0001, **Fig. 3N**, **O**), indicative of a spreading dysfunction in CD37 deficient platelets. These data indicate that *Cd37*$^{-/-}$ platelets have restricted cytoskeletal reorganization following adhesion and are consistent with CD37 regulating αIIbβ3 integrin-associated signaling responses.

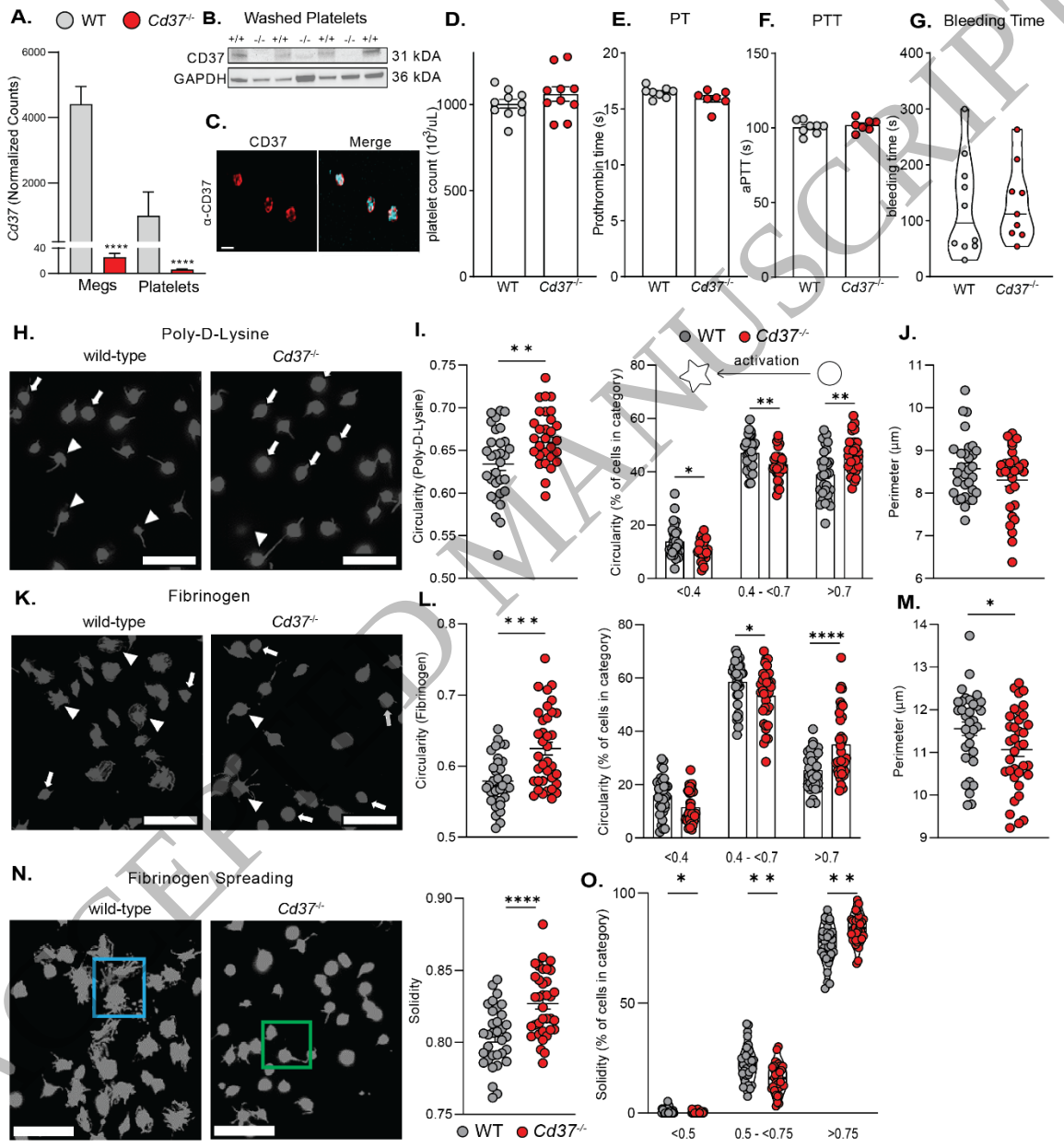

Figure 3. Absence of CD37 Impairs Platelet Spreading and Activation with no Alterations to Hemostasis

(A) Wild-type and *Cd37*$^{-/-}$ mouse megakaryocyte and platelet *Cd37* expression as determined by RNA-seq. Normalized expression levels are shown. n = 4-6 samples per group. Mean ± SEM, ****p<0.001 by Student's t-test. **(B)** Representative western blot of CD37 and GAPDH of platelets lysates from wild-type and *Cd37*$^{-/-}$ mice. **(C)** Super-resolution microscopy images of

platelets immunostained with CD37 (red) and actin filaments (cyan) were reconstructed using the structured illumination microscopy (SIM^2) algorithm. Scale bar = 2 µm. **(D)** Circulating platelet counts, **(E)** prothrombin (PT) and **(F)** partial thromboplastin time (PTT) measured in whole blood (measured by Heska COAG+), and **(G)** time to tail bleeding cessation in wild-type and *Cd37*$^{-/-}$ mice. Spreading of *Cd37*$^{-/-}$ and wild-type platelets and circularity of adherent platelets assessed by image analysis. Images of cells were assessed by quantification of cell circularity where a value <0.4 equates to a spread/activated platelet (indicated by arrowheads), and >0.7 equates to a minimally spread/activated platelet (indicated by arrows). Platelet spreading on **(H)** poly-D-lysine (50 µg/mL), **(I)** circularity of adherent platelets and the frequency distribution of circularity, categorized as <0.4, 0.4-<0.7, and >0.7, and **(J)** platelet perimeter. Spreading of *Cd37*$^{-/-}$ and wild-type platelets on **(K)** fibrinogen (100 µg/mL), **(L)** circularity of adherent platelets, and the frequency distribution categorized as <0.4, 0.4-<0.7, and >0.7, and **(M)** platelet perimeter. **(N)** Platelet solidity following spreading on fibrinogen (100 µg/mL) for 45 min, and the **(O)** frequency distribution. Grey circles, wild-type mice (n = 4-5); red circles, *Cd37*$^{-/-}$ mice (n = 4-5). At least 5 images and a total of 650 cells were analyzed per mouse. Data are shown as mean ± SEM *p<0.05, **p<0.01, ***p<0.005, ****p<0.0001 as determined by the student's t-test. Scale bar = 10 µm.

CD37 Deficiency Reduces Platelet Activation Responses and is Protective From Thrombosis in Mice

In whole blood, expression of activated integrin αIIbβ3 is unaltered between *Cd37*$^{-/-}$ and wild-type platelets under resting conditions; however, following stimulation with PAR4-AP, JON/A expression is significantly attenuated on *Cd37*$^{-/-}$ platelets relative to controls (p<0.0001, **Fig. 4A**). PAR4-AP stimulation did not alter *Cd37*$^{-/-}$ platelet expression of P-selectin (**Fig. 4B**); however, dense granule release was significantly decreased (p<0.05, **Fig. 4C**). Furthermore, *Cd37*$^{-/-}$ platelets had reduced activation response to U46619+ADP and epinephrine (**SFig. 5**). To assess the functional consequence of reduced platelet adhesion and activation responses of platelets from *Cd37*$^{-/-}$ mice, we next performed the $FeCl_3$ thrombosis model to induce platelet-rich thrombi formation within the carotid artery. Lethally irradiated wild-type mice were transplanted with bone marrow from wild-type or *Cd37*$^{-/-}$ mice, a $FeCl_3$ patch was applied to the carotid artery, and time to vessel occlusion was monitored. Consistent with a role for CD37 in regulating thrombosis-relevant platelet activation responses, chimeric mice that received *Cd37*$^{-/-}$ bone marrow experienced a significantly increased time to vessel occlusion (p<0.05, **Fig. 4D, E**), and area under the curve (p<0.005, **Fig. 4F**). These data indicate that the absence of CD37 significantly delays the time to thrombosis formation.

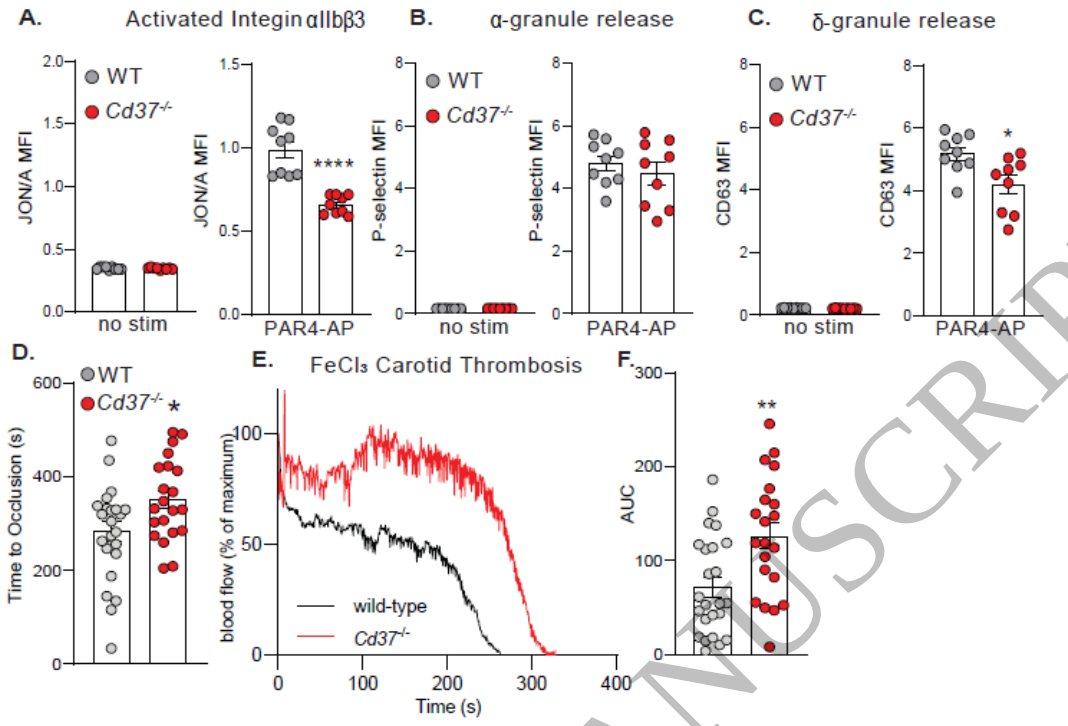

Figure 4. CD37 Deficiency Is Protective From Thrombosis
Platelet surface expression of the activation markers **(A)** activated integrin αIIbβ3, **(B)** P-selectin, and **(C)** CD63 following incubation with PBS (no stim) or PAR4-activating peptide (PAR4-AP, 50 μM) for 15 min. Grey circles, wild-type mice (n = 10); red circles, *Cd37*$^{-/-}$ mice (n = 12). $FeCl_3$ carotid thrombosis model in wild-type and *Cd37*$^{-/-}$ mice. **(D)** Mean time to vessel occlusion as measured by a flow probe, **(E)** representative carotid artery blood flow following removal of $FeCl_3$ patch and **(F)** area under the curve (AUC) analysis. Grey circles, wild-type; red circles, *Cd37*$^{-/-}$ mice (n = 10-12 mice per group). Mean ± SEM, *p<0.05, **p<0.05, ****p<0.0001 by Student's t-test.

To assess the contribution of CD37 to human platelet activation responses, we utilized CRISPR-Cas9 to generate CD37 knock-down human CD34^{+}-derived megakaryocytes (**Fig. 5A**, **SFig. 6, SFig. 7**). In the resting state, the absence of CD37 did not alter traditional platelet functional responses including the basal expression of PAC-1, P-selectin, or CD63 (**Fig. 5B-D**). However, following thrombin activation expression of PAC-1, P-selectin and CD63 is significantly attenuated in the CD37 knock-down megakaryocytes. These studies support that inhibition of CD37 impairs human platelet activation.

Platelet CD37 is Increased During Acute MI and Associates with Stress

To clinically validate the relationship between platelet *CD37* and thrombosis, we profiled platelets of patients who presented with a MI (n = 40) relative to those referred for coronary angiography without a MI (n = 38, Demographics **STable 5**). In those experiencing a MI, *CD37* expression was significantly higher (p=0.003, **Fig. 5E**). Within the MI cohort, a subset of patients

was administered a validated stress questionnaire at hospital admission [perceived stress scale 4 (PSS-4)].[64] When stratified by stress level, platelet *CD37* expression was significantly higher in patients with "high stress" versus "low stress" (p=0.002, **Fig. 5F)** and positively correlated with reported stress levels (**Fig. 5G**), supporting a mechanistic link between stress, thrombosis, and platelet *CD37*. Within the MI cohort, 16 patients returned post the acute event (approximately 3 months), and their platelet RNA was reassessed. At follow-up, we found that platelet *CD37* levels were significantly reduced relative to the time of the acute MI (p=0.012, **Fig. 5H**), consistent with reduced stress levels and platelet hyperreactivity post-MI.

To identify transcriptional regulators of platelet *CD37,* we integrated the RNA-seq data collected from our high-stress human cohort (**Fig. 2C**), and MI cohort. Upstream transcription factor regulators were predicted with Ingenuity Pathway Analysis (IPA), and those enriched in platelets compared between the cohorts (p<0.01, NES>1.50). This analysis revealed nine common transcription factors (**Fig. 5I**), including serum response factor (SRF), specific protein 1 (SP1), runt-related transcription factor 1 (RUNX1), and GATA binding factor 1 (GATA1). Mining of ENCODE chromatin immunoprecipitation sequencing (ChIP-seq) data for CD37 promoter transcription factor occupancy revealed that two of the nine candidate transcription factors were previously shown to bind to the CD37 promoter; SRF and SP1. Furthermore, two additional transcription factors identified, myocardin-related transcription factor (MRTF)-A and MRTF-B, are known SRF key activators[65] – however no ChIP-seq data for these transcription factors is currently available in the ENCODE database. SRF/MRTFs are master regulators of the actin cytoskeleton, with numerous SRF target genes encoding proteins related to actin dynamics, lamellipodia/filopodia formation, and integrin-cytoskeletal coupling.[66] Further evidence for the role of the SRF-MRTF axis is illustrated by the upregulation of multiple actin-associated SRF target genes in platelets from high-stress subjects, e.g., *TUBB6, P2RX1*, *WDR1*, *MYH9*, *ACTIN1*, *ITGA2B* (**Fig. 5J**).

Dual Anti-platelet Therapy Reduces CD37

Anti-platelet therapy is the mainstay approach to prevent adverse cardiovascular events precipitated by hyperreactive platelets. We therefore investigated whether aspirin or $P2Y_{12}$ inhibition alters *CD37* expression and thus may represent a potential pharmacological approach to reduce CD37-mediated platelet hyperreactivity. Human $CD34^+$ cell-derived megakaryocytes, to model platelet transcriptomic responses, from four independent donors were treated with aspirin, the $P2Y_{12}$ inhibitor AZD1283, or both drugs for 24 hours, and expression of *CD37* was assessed (**Fig. 5K**). Whereas megakaryocyte exposure to aspirin did not significantly alter

CD37 expression, and AZD1283 treatment led to 31.1% decline in expression, simultaneous treatment with both drugs resulted in a significant 42% reduction in megakaryocyte *CD37* expression ($p<0.01$, **Fig. 5L**). Furthermore, transcription factor regulator analysis in megakaryocytes treated with aspirin and AZD1283 found a significant reduction in SRF and SP-1 enrichment (7.56×10^{-6} and 8.42×10^{-5}, respectively, data not shown).

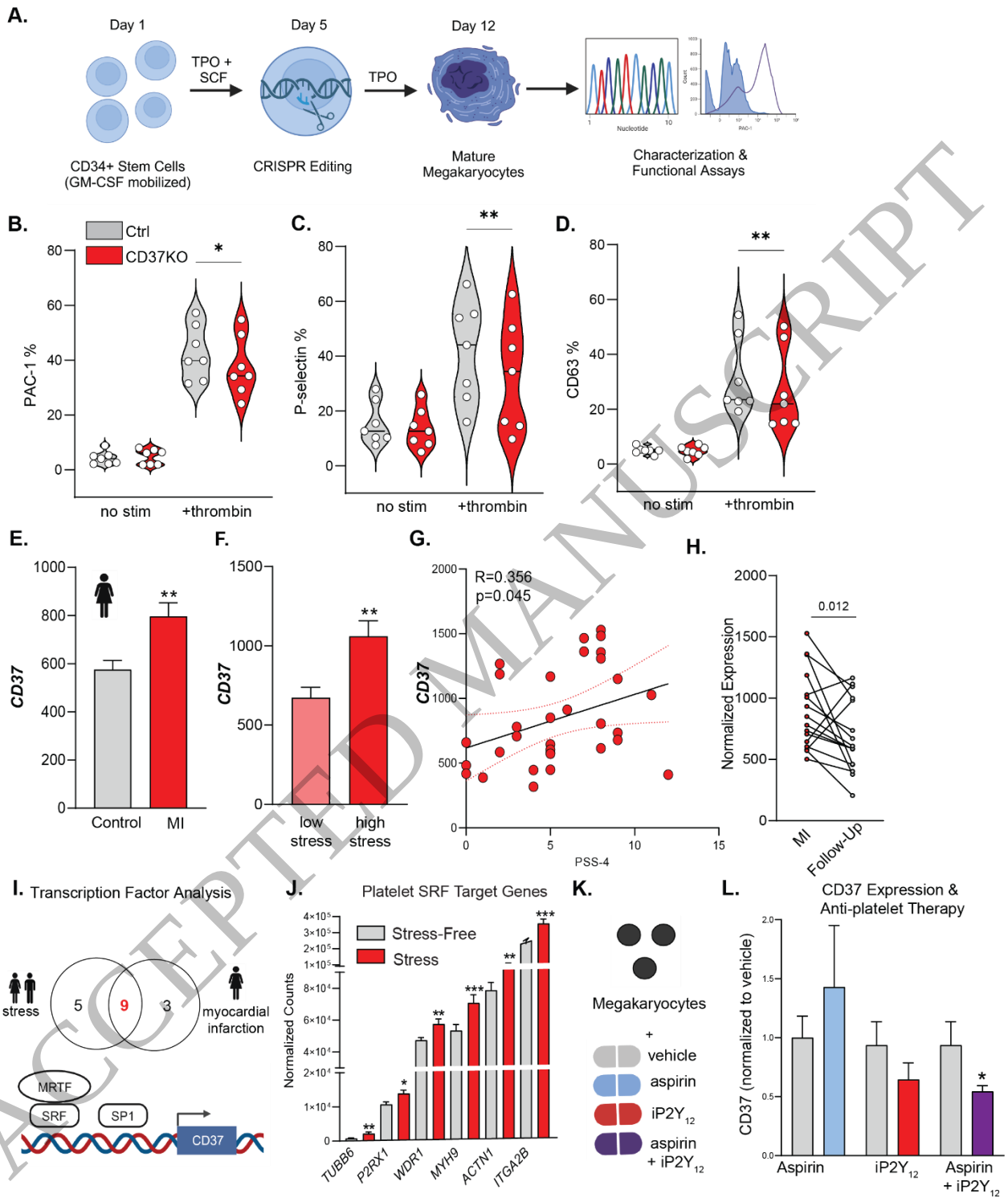

Figure 5. Platelet CD37 is Increased During Myocardial Infarction and Associates with Stress Levels

(A) Schematic overview of the generation of mature human megakaryocytes from CD34⁺ stem cells. Megakaryocyte expression of **(B)** activated αIIb/β3 (PAC-1), **(C)** P-selectin and **(D)** CD63 in unstimulated (no stim) or following treatment with thrombin (0.5 U/mL) for 15 minutes (n = 7 unique stem cell donors). Data are shown as a violin plot. P-values were calculated using a

paired Student t-test.*P < 0.05; **P < 0.01. Women electively referred for invasive coronary angiography with or without acute coronary syndrome were enrolled in the Heart Attack Research Program (HARP) study. **(E)** MI patients and controls had blood collected for platelet transcriptome and activity measures at the time of coronary angiography. Platelet *CD37* expression in control (n = 38) and MI (n = 40) subjects as determined by RNA-seq, **(F)** stratification of MI subjects into low (PSS-4<6) and high (PSS-4≥6) stress and platelet *CD37* expression. Mean ± SEM, **p<0.01 by Student's t-test. **(G)** Correlation between self-reported stress level and platelet *CD37* expression. **(H)** Platelet *CD37* expression at initial study entry and 3 months post-MI (n = 16 paired samples). **(I)** Overlap of predicted upstream transcriptional regulators as determined by Ingenuity Pathway Analysis of genes differentially expressed in platelets from stressed versus stress-free control subjects or women experiencing a myocardial infarction. ENCODE ChIP-Seq assessment of common CD37 regulators identified to by Ingenuity Pathway Analysis. **(J)** Normalized expression counts of serum response factor (SRF) regulated genes in platelets from stressed versus stress-free control subjects. **(K)** $CD34^{+}$-derived megakaryocytes were treated with 100 μM aspirin, 5 μM AZD1283 ($P2Y_{12}$ inhibitor), or both aspirin and AZD1283 for 24 hours. **(L)** Megakaryocytes CD37 expression following treatment with anti-platelet therapies or vehicle control. Mean ± SEM, *p<0.05, **p<0.01, ***p<0.005 by Student's t-test.

DISCUSSION

We report that platelets from both stressed humans and mice are hyperreactive and that this platelet phenotype significantly contributes to heightened thrombotic risk. Our findings identify a mechanism by which stress-mediated thrombosis occurs and describe the role platelets play as critical mediators of thrombosis. By integrating platelet phenotyping and transcriptomic analyses from stressed humans and mice, we identify CD37 as a previously unrecognized regulator of platelet activation responses. We demonstrate that CD37 positively associates with αIIbβ3-mediated platelet aggregation and that CD37-deficient platelets have a defect in integrin αIIbβ3-mediated signaling processes as indicated by reduced platelet activation responses and reduced platelet spreading on fibrinogen. Furthermore, deficiency of CD37 is protective against thrombosis and stress-accelerated thrombosis, while CD37-deficient mice have normal coagulation and hemostatic parameters. Collectively, our data identify a new regulator of platelet activation responses, CD37, and highlight how, in the setting of platelet hyperreactivity, including physiological stress and MI, platelet CD37 positively associates with thrombotic risk.

Chronic stress is associated with an increased risk of cardiovascular disease [67], with an attributable risk comparable to other major cardiovascular risk factors (e.g. diabetes, hypertension).[2] To date, most studies have investigated how stress contributes to and accelerates atherosclerosis.[7, 68-70] Despite the robust association between stress and adverse thrombotic events, less is known about how psychological stress translates into increased cardiovascular event (e.g., thrombotic) risk.[2, 4, 7-9] With approximately a third of US adults

reporting overwhelming stress levels most days,[10] defining the mechanisms by which psychosocial stress accelerates cardiovascular events and thrombotic risk is necessary to reduce stress-associated morbidity and mortality.

Platelets are key contributors to the progression of cardiovascular disease and the development of cardiovascular events.[11-13] Stress has been shown to increase platelet activation and secretion [14-16, 18] and alterations in platelet activity due to mental stress may explain, in part, the stress-cardiovascular event risk relationship.[19, 20] Consistent with these findings, in our current study, we report increased circulating levels of leukocyte-platelet aggregates, a marker of platelet hyperreactivity, in subjects with high psychological stress (**Fig. 1B**), a finding that was recapitulated in our mouse model of chronic variable stress (**Fig. 1F**). Furthermore, analogous to humans, we demonstrate in our mouse model that increased platelet reactivity translates to an increased thrombotic risk (**Fig. 1H-K**). To investigate platelet-specific mechanisms contributing to stress-mediated hyperreactivity, we integrated platelet RNA-seq data from human and mouse stress cohorts (**Fig. 2A**-**D**) and assessed the functional response of identified candidates by platelet aggregation to submaximal epinephrine stimulation (**Fig. 2E**). This analysis identified platelet CD37 as a regulator of platelet activation responses, upregulated by psychosocial stress (**Fig. 2E**, **F, H**). Further, we found CD37 to be upregulated in a cohort of patients with acute MI and confirmed its association with stress levels (**Fig. 5E**-**H**). Although our study is the first to identify the upregulation of platelet CD37 in patients with high psychosocial stress and during MI, there is evidence that CD37 may also be upregulated on alternative cell types in those with chronic coronary syndromes and post-ischemia [71-73].

To date, there are no approved therapeutic approaches to reduce stress-associated platelet hyperreactivity. However, given that anti-platelet therapy is the mainstay approach to prevent adverse cardiovascular events, we investigated the effect of aspirin or $P2Y_{12}$ inhibition therapy on megakaryocyte *CD37* expression. Results from these studies indicate that megakaryocytes/platelet *CD37* is suppressed by dual aspirin and $P2Y_{12}$ inhibitor therapy (**Fig. 5K**, **L**). Given that several psychosocial stress intervention trials indicate that stress reduction can suppress cardiovascular event risk to a magnitude of reduction comparable to that of other therapies (e.g., lipid-lowering, antiplatelet),[74] future studies designed to investigate stress-mitigating lifestyle factors should consider the impact of these strategies to platelet activity and the transcriptome.

CD37 is a tetraspanin, a family of four transmembrane proteins expressed on cell surfaces and subcellular compartments. [75, 76] Their major role is the spatial organization of proteins in the cell membrane, where tetraspanins direct other proteins into regulated, signal-transducing microdomains known as tetraspanin-enriched microdomains.[75, 77] CD37 has been identified at the proteome level in several,[31, 32, 78] but not all platelet proteomic studies.[79] Our platelet findings are consistent with previous studies in different cell types showing how tetraspanins act as cell membrane organizers, facilitating cell-signaling events by recruiting factors including integrins and G-protein-coupled receptors to cell membranes. [75, 80] Other molecules in this class have previously been investigated in platelets, with different tetraspanins varying in their capacity to modulate platelet function, fine-tune hemostasis and bleeding risk. CD9, CD82, and CD63 deficiency have mild effects on platelet function,[81] while loss of Tspan32[82] and CD151[83] results in excessive bleeding due to defective integrin αIIbβ3 activation. In contrast, our data indicate that deficiency of CD37 does not alter hemostasis despite reducing the platelet activation profile and risk of thrombosis. Tetraspanin deficiency and defective integrin αIIbβ3 activation is hypothesized to occur due to either loss of direct tetraspanin- αIIbβ3 primary complexes, or by impairing a tetraspanin-associated protein that regulates αIIbβ3 activation via a secondary interaction.[82, 83] Future studies will address how CD37 directly regulates integrin αIIbβ3 mediated signaling events. Furthermore, given the reports that CD37 is required for CLEC-2 recruitment in the cell membrane in dendritic cells, future studies should address this interaction in platelets.[62]

CD37 has documented functions in many different leukocyte lineages, including B cells,[48, 58] T cells,[59] dendritic cells,[60-62] neutrophils,[56] and monocytes;[57] however, its function in platelets has not previously been investigated. CD37 is integral to modulating cytoskeletal-dependent parameters in other cell types, including actin polymerization, cell spreading, and polarization.[56, 60] Cytoskeletal-dependent processes are key for platelet shape change and subsequent activation.[84] Indeed, we found that CD37 deficiency altered platelet adhesion, spreading, and subsequent agonist-mediated activation responses. Following adhesion to fibrinogen, *Cd37*$^{-/-}$ platelets underwent a minimal change in morphology, maintaining a more rounded shape and forming a smaller number of filopodia (**Fig. 3N**). Furthermore, consistent with CD37 regulating αIIbβ3 integrin-associated signaling responses, CD37-deficient platelets showed decreased expression of activated αIIbβ3 integrin and dense granule release following agonist activation (**Fig. 4A**-**C**). The physiological outcomes of these reduced signaling events translate to decreased thrombosis susceptibility in *Cd37*$^{-/-}$ mice (**Fig. 4D**-**F**). The current study utilized

chimeric mice that received either wild-type or *Cd37*$^{-/-}$ bone marrow; thus, the contribution of leukocyte CD37 to thrombosis risk cannot be ruled out as a contributing mechanism. However, we did not detect a significant difference in CD37 expression on leukocytes, neutrophils, or monocytes between stressed and nonstressed control mice (**SFig. 2C**-**E**). Future studies in platelet-specific knockout mice (e.g., PF4-cre, Gp1ba-cre) will delineate the contribution of platelets and leukocytes to thrombotic risk.

CD37 is the only tetraspanin targeted therapeutically in humans, with several monoclonal antibodies and chimeric antigen receptor-based immunotherapies developed for treating B cell-derived lymphomas and leukemia.[85, 86] If and how these therapies alter platelet function remains to be established, and whether these approaches alter thrombotic risk, analogous to therapies that directly target integrin αIIbβ3. The potential success of the clinical applicability for CD37-targeting approaches to suppress thrombotic risk is supported by our data demonstrating that CD37 deficiency does not alter hemostatic or coagulation parameters or increase risk bleeding risk in mice (**Fig. 5**), a drawback of current anti-platelet therapies used for cardiovascular prevention.[27]

Collectively, our data define a new mechanism for platelet hyperreactivity regulated by CD37 and raises the possibility that developing antiplatelet therapeutics targeting platelet CD37 may attenuate platelet-mediated adverse cardiovascular events.

Funding: National Institutes of Health (R01HL167917 (TJB), R35HL144993 (JSB), R01HL172335 & R01HL172365 (KJM), R56HL155528 (KR), R01HL163019 & R01HL160808 (RAC)), American Heart Association (16SFRN2873002 (JSB), 16SFRN28850003 (TS), SFRN28730004, SFRN28730006 (HRR), 19CDA34630066, 23SCEFIA1153739 (CvS))

Conflict of interest disclosure: HR has received in kind donations for research from Abbott Vascular and Siemens (related), Philips and SHL Telemedicine (unrelated). All other authors declare that they have no competing interests.

Data availability: Sequencing data is available on GSE242369 and GSE242369. All other output is supplied as supplementary information. Additional data, results, or code is available upon reasonable request.

Patient consent statement: All participants included in the study provided informed consent.

Clinical trial registration: NCT02106429, NCT03022552

Author contributions:

Conceptualization: TJB, EC, KJM, JSB
Methodology: TJB, IP, CH, EC, KJM, JSB, KR, MAS
Investigation: TJB, EC, MC, CH, IP, MAS, KD, MD, AHL, CvS, EF, BB
Funding acquisition: TJB, JSB, KJM, HR
Supervision: TJB
Writing – original draft: TJB, JSB
Writing – review & editing: TS, HR, JH, KR, CvS, KJM, MAS, RAC

List of Supplementary Materials

SFigures. 1-7

STables. 1-5

References

1. Virani SS, Alonso A, Aparicio HJ, Benjamin EJ, Bittencourt MS, Callaway CW, Carson AP, Chamberlain AM, Cheng S, Delling FN, Elkind MSV, Evenson KR, Ferguson JF, Gupta DK, Khan SS, Kissela BM, Knutson KL, Lee CD, Lewis TT, Liu J, Loop MS, Lutsey PL, Ma J, Mackey J, Martin SS, Matchar DB, Mussolino ME, Navaneethan SD, Perak AM, Roth GA, Samad Z, Satou GM, Schroeder EB, Shah SH, Shay CM, Stokes A, VanWagner LB, Wang NY, Tsao CW, American Heart Association Council on E, Prevention Statistics C and Stroke Statistics S. Heart Disease and Stroke Statistics-2021 Update: A Report From the American Heart Association. *Circulation*. 2021;143:e254-e743.
2. Rosengren A, Hawken S, Ounpuu S, Sliwa K, Zubaid M, Almahmeed WA, Blackett KN, Sitthi-amorn C, Sato H, Yusuf S and investigators I. Association of psychosocial risk factors with risk of acute myocardial infarction in 11119 cases and 13648 controls from 52 countries (the INTERHEART study): case-control study. *Lancet*. 2004;364:953-62.
3. Anand SS, Islam S, Rosengren A, Franzosi MG, Steyn K, Yusufali AH, Keltai M, Diaz R, Rangarajan S, Yusuf S and Investigators I. Risk factors for myocardial infarction in women and men: insights from the INTERHEART study. *Eur Heart J*. 2008;29:932-40.
4. Yusuf S, Hawken S, Ounpuu S, Dans T, Avezum A, Lanas F, McQueen M, Budaj A, Pais P, Varigos J, Lisheng L and Investigators IS. Effect of potentially modifiable risk factors associated with myocardial infarction in 52 countries (the INTERHEART study): case-control study. *Lancet*. 2004;364:937-52.
5. Fleshner M and Crane CR. Exosomes, DAMPs and miRNA: Features of Stress Physiology and Immune Homeostasis. *Trends Immunol*. 2017;38:768-76.
6. Powell ND, Sloan EK, Bailey MT, Arevalo JM, Miller GE, Chen E, Kobor MS, Reader BF, Sheridan JF and Cole SW. Social stress up-regulates inflammatory gene expression in the leukocyte transcriptome via beta-adrenergic induction of myelopoiesis. *Proc Natl Acad Sci U S A*. 2013;110:16574-9.
7. Heidt T, Sager HB, Courties G, Dutta P, Iwamoto Y, Zaltsman A, von Zur Muhlen C, Bode C, Fricchione GL, Denninger J, Lin CP, Vinegoni C, Libby P, Swirski FK, Weissleder R and Nahrendorf M. Chronic variable stress activates hematopoietic stem cells. *Nat Med*. 2014;20:754-8.
8. Arnold SV, Smolderen KG, Buchanan DM, Li Y and Spertus JA. Perceived stress in myocardial infarction: long-term mortality and health status outcomes. *J Am Coll Cardiol*. 2012;60:1756-63.

9. Jennings JR, Kamarck TW, Everson-Rose SA, Kaplan GA, Manuck SB and Salonen JT. Exaggerated blood pressure responses during mental stress are prospectively related to enhanced carotid atherosclerosis in middle-aged Finnish men. *Circulation*. 2004;110:2198-203.
10. Association AP. Stress in America Survey. 2022.
11. Barrett TJ, Schlegel M, Zhou F, Gorenchtein M, Bolstorff J, Moore KJ, Fisher EA and Berger JS. Platelet regulation of myeloid suppressor of cytokine signaling 3 accelerates atherosclerosis. *Sci Transl Med*. 2019;11.
12. Allen N, Barrett TJ, Guo Y, Nardi M, Ramkhelawon B, Rockman CB, Hochman JS and Berger JS. Circulating monocyte-platelet aggregates are a robust marker of platelet activity in cardiovascular disease. *Atherosclerosis*. 2019;282:11-8.
13. Nording H, Baron L and Langer HF. Platelets as therapeutic targets to prevent atherosclerosis. *Atherosclerosis*. 2020;307:97-108.
14. Markovitz JH and Matthews KA. Platelets and coronary heart disease: potential psychophysiologic mechanisms. *Psychosom Med*. 1991;53:643-68.
15. Wallen NH, Held C, Rehnqvist N and Hjemdahl P. Effects of mental and physical stress on platelet function in patients with stable angina pectoris and healthy controls. *Eur Heart J*. 1997;18:807-15.
16. Naesh O, Haedersdal C, Hindberg I and Trap-Jensen J. Platelet activation in mental stress. *Clin Physiol*. 1993;13:299-307.
17. Jiang W, Boyle SH, Ortel TL, Samad Z, Velazquez EJ, Harrison RW, Wilson J, Kuhn C, Williams RB, O'Connor CM and Becker RC. Platelet aggregation and mental stress induced myocardial ischemia: Results from the Responses of Myocardial Ischemia to Escitalopram Treatment (REMIT) study. *Am Heart J*. 2015;169:496-507 e1.
18. Levine SP, Towell BL, Suarez AM, Knieriem LK, Harris MM and George JN. Platelet activation and secretion associated with emotional stress. *Circulation*. 1985;71:1129-34.
19. Kivimaki M and Steptoe A. Effects of stress on the development and progression of cardiovascular disease. *Nat Rev Cardiol*. 2018;15:215-29.
20. Osborne MT, Shin LM, Mehta NN, Pitman RK, Fayad ZA and Tawakol A. Disentangling the Links Between Psychosocial Stress and Cardiovascular Disease. *Circ Cardiovasc Imaging*. 2020;13:e010931.
21. Eicher JD, Wakabayashi Y, Vitseva O, Esa N, Yang Y, Zhu J, Freedman JE, McManus DD and Johnson AD. Characterization of the platelet transcriptome by RNA sequencing in patients with acute myocardial infarction. *Platelets*. 2016;27:230-9.
22. Montenont E, Echagarruga C, Allen N, Araldi E, Suarez Y and Berger JS. Platelet WDR1 suppresses platelet activity and is associated with cardiovascular disease. *Blood*. 2016;128:2033-42.
23. Healy AM, Pickard MD, Pradhan AD, Wang Y, Chen Z, Croce K, Sakuma M, Shi C, Zago AC, Garasic J, Damokosh AI, Dowie TL, Poisson L, Lillie J, Libby P, Ridker PM and Simon DI. Platelet expression profiling and clinical validation of myeloid-related protein-14 as a novel determinant of cardiovascular events. *Circulation*. 2006;113:2278-84.
24. Dann R, Hadi T, Montenont E, Boytard L, Alebrahim D, Feinstein J, Allen N, Simon R, Barone K, Uryu K, Guo Y, Rockman C, Ramkhelawon B and Berger JS. Platelet-Derived MRP-14 Induces Monocyte Activation in Patients With Symptomatic Peripheral Artery Disease. *J Am Coll Cardiol*. 2018;71:53-65.
25. Schubert S, Weyrich AS and Rowley JW. A tour through the transcriptional landscape of platelets. *Blood*. 2014;124:493-502.
26. Davizon-Castillo P, Rowley JW and Rondina MT. Megakaryocyte and Platelet Transcriptomics for Discoveries in Human Health and Disease. *Arterioscler Thromb Vasc Biol*. 2020;40:1432-40.

27. Cofer LB, Barrett TJ and Berger JS. Aspirin for the Primary Prevention of Cardiovascular Disease: Time for a Platelet-Guided Approach. *Arterioscler Thromb Vasc Biol*. 2022;42:1207-16.
28. In 't Veld S, Arkani M, Post E, Antunes-Ferreira M, D'Ambrosi S, Vessies DCL, Vermunt L, Vancura A, Muller M, Niemeijer AN, Tannous J, Meijer LL, Le Large TYS, Mantini G, Wondergem NE, Heinhuis KM, van Wilpe S, Smits AJ, Drees EEE, Roos E, Leurs CE, Tjon Kon Fat LA, van der Lelij EJ, Dwarshuis G, Kamphuis MJ, Visser LE, Harting R, Gregory A, Schweiger MW, Wedekind LE, Ramaker J, Zwaan K, Verschueren H, Bahce I, de Langen AJ, Smit EF, van den Heuvel MM, Hartemink KJ, Kuijpers MJE, Oude Egbrink MGA, Griffioen AW, Rossel R, Hiltermann TJN, Lee-Lewandrowski E, Lewandrowski KB, De Witt Hamer PC, Kouwenhoven M, Reijneveld JC, Leenders WPJ, Hoeben A, Verdonck-de Leeuw IM, Leemans CR, Baatenburg de Jong RJ, Terhaard CHJ, Takes RP, Langendijk JA, de Jager SC, Kraaijeveld AO, Pasterkamp G, Smits M, Schalken JA, Lapinska-Szumczyk S, Lojkowska A, Zaczek AJ, Lokhorst H, van de Donk N, Nijhof I, Prins HJ, Zijlstra JM, Idema S, Baayen JC, Teunissen CE, Killestein J, Besselink MG, Brammen L, Bachleitner-Hofmann T, Mateen F, Plukker JTM, Heger M, de Mast Q, Lisman T, Pegtel DM, Bogaard HJ, Jassem J, Supernat A, Mehra N, Gerritsen W, de Kroon CD, Lok CAR, Piek JMJ, Steeghs N, van Houdt WJ, Brakenhoff RH, Sonke GS, Verheul HM, Giovannetti E, Kazemier G, Sabrkhany S, Schuuring E, Sistermans EA, Wolthuis R, Meijers-Heijboer H, Dorsman J, Oudejans C, Ylstra B, Westerman BA, van den Broek D, Koppers-Lalic D, Wesseling P, Nilsson RJA, Vandertop WP, Noske DP, Tannous BA, Sol N, Best MG and Wurdinger T. Detection and localization of early- and late-stage cancers using platelet RNA. *Cancer Cell*. 2022;40:999-1009 e6.
29. Best MG, In 't Veld S, Sol N and Wurdinger T. RNA sequencing and swarm intelligence-enhanced classification algorithm development for blood-based disease diagnostics using spliced blood platelet RNA. *Nat Protoc*. 2019;14:1206-34.
30. Marcantoni E, Allen N, Cambria MR, Dann R, Cammer M, Lhakhang T, O'Brien MP, Kim B, Worgall T, Heguy A, Tsirigos A and Berger JS. Platelet Transcriptome Profiling in HIV and ATP-Binding Cassette Subfamily C Member 4 (ABCC4) as a Mediator of Platelet Activity. *JACC Basic Transl Sci*. 2018;3:9-22.
31. Burkhart JM, Vaudel M, Gambaryan S, Radau S, Walter U, Martens L, Geiger J, Sickmann A and Zahedi RP. The first comprehensive and quantitative analysis of human platelet protein composition allows the comparative analysis of structural and functional pathways. *Blood*. 2012;120:e73-82.
32. Huang J, Swieringa F, Solari FA, Provenzale I, Grassi L, De Simone I, Baaten C, Cavill R, Sickmann A, Frontini M and Heemskerk JWM. Assessment of a complete and classified platelet proteome from genome-wide transcripts of human platelets and megakaryocytes covering platelet functions. *Sci Rep*. 2021;11:12358.
33. Tomlinson MG. Platelet tetraspanins: small but interesting. *J Thromb Haemost*. 2009;7:2070-3.
34. Malik AO, Peri-Okonny P, Gosch K, Thomas M, Mena C, Hiatt WR, Jones PG, Provance JB, Labrosciano C, Jelani QU, Spertus JA and Smolderen KG. Association of Perceived Stress Levels With Long-term Mortality in Patients With Peripheral Artery Disease. *JAMA Netw Open*. 2020;3:e208741.
35. Born GV. Aggregation of blood platelets by adenosine diphosphate and its reversal. *Nature*. 1962;194:927-9.
36. Barrett TJ, Bilaloglu S, Cornwell M, Burgess HM, Virginio VW, Drenkova K, Ibrahim H, Yuriditsky E, Aphinyanaphongs Y, Lifshitz M, Xia Liang F, Alejo J, Smith G, Pittaluga S, Rapkiewicz AV, Wang J, Iancu-Rubin C, Mohr I, Ruggles K, Stapleford KA, Hochman J and Berger JS. Platelets contribute to disease severity in COVID-19. *J Thromb Haemost*. 2021;19:3139-53.

37. Barrett TJ, Cornwell M, Myndzar K, Rolling CC, Xia Y, Drenkova K, Biebuyck A, Fields AT, Tawil M, Luttrell-Williams E, Yuriditsky E, Smith G, Cotzia P, Neal MD, Kornblith LZ, Pittaluga S, Rapkiewicz AV, Burgess HM, Mohr I, Stapleford KA, Voora D, Ruggles K, Hochman J and Berger JS. Platelets amplify endotheliopathy in COVID-19. *Sci Adv*. 2021;7:eabh2434.
38. igordot/sns [computer program]. 2020.
39. Dobin A, Davis CA, Schlesinger F, Drenkow J, Zaleski C, Jha S, Batut P, Chaisson M and Gingeras TR. STAR: ultrafast universal RNA-seq aligner. *Bioinformatics*. 2013;29:15-21.
40. Liao Y, Smyth GK and Shi W. featureCounts: an efficient general purpose program for assigning sequence reads to genomic features. *Bioinformatics*. 2014;30:923-30.
41. Andrews. Babraham Bioinformatics - FastQC A Quality Control tool for High Throughput Sequence Data.
42. Gu Z, Eils R and Schlesner M. Complex heatmaps reveal patterns and correlations in multidimensional genomic data. *Bioinformatics*. 2016;32:2847-9.
43. Gu Z, Eils R and Schlesner M. Complex heatmaps reveal patterns and correlations in multidimensional genomic data. *Bioinformatics*. 2016;32:2847-9.
44. Wickham H. *ggplot2: Elegant Graphics for Data Analysis*: Springer-Verlag New York; 2016.
45. Langfelder P and Horvath S. WGCNA: an R package for weighted correlation network analysis. *BMC Bioinformatics*. 2008;9:559.
46. Sowa MA, Sun H, Wang TT, Virginio VW, Schlamp F, El Bannoudi H, Cornwell M, Bash H, Izmirly PM, Belmont HM, Ruggles KV, Buyon JP, Voora D, Barrett TJ and Berger JS. Inhibiting the P2Y(12) Receptor in Megakaryocytes and Platelets Suppresses Interferon-Associated Responses. *JACC Basic Transl Sci*. 2024;9:1126-40.
47. Chen X, Zhong S, Hou Y, Cao R, Wang W, Li D, Dai Q, Kim D and Xi P. Superresolution structured illumination microscopy reconstruction algorithms: a review. *Light Sci Appl*. 2023;12:172.
48. Knobeloch KP, Wright MD, Ochsenbein AF, Liesenfeld O, Lohler J, Zinkernagel RM, Horak I and Orinska Z. Targeted inactivation of the tetraspanin CD37 impairs T-cell-dependent B-cell response under suboptimal costimulatory conditions. *Mol Cell Biol*. 2000;20:5363-9.
49. Barrett TJ, Corr EM, van Solingen C, Schlamp F, Brown EJ, Koelwyn GJ, Lee AH, Shanley LC, Spruill TM, Bozal F, de Jong A, Newman AAC, Drenkova K, Silvestro M, Ramkhelawon B, Reynolds HR, Hochman JS, Nahrendorf M, Swirski FK, Fisher EA, Berger JS and Moore KJ. Chronic stress primes innate immune responses in mice and humans. *Cell Rep*. 2021;36:109595.
50. Rowley JW, Chappaz S, Corduan A, Chong MM, Campbell R, Khoury A, Manne BK, Wurtzel JG, Michael JV, Goldfinger LE, Mumaw MM, Nieman MT, Kile BT, Provost P and Weyrich AS. Dicer1-mediated miRNA processing shapes the mRNA profile and function of murine platelets. *Blood*. 2016;127:1743-51.
51. Bonnard T and Hagemeyer CE. Ferric Chloride-induced Thrombosis Mouse Model on Carotid Artery and Mesentery Vessel. *J Vis Exp*. 2015:e52838.
52. Li W, McIntyre TM and Silverstein RL. Ferric chloride-induced murine carotid arterial injury: A model of redox pathology. *Redox Biol*. 2013;1:50-5.
53. Fidler TP, Marti A, Gerth K, Middleton EA, Campbell RA, Rondina MT, Weyrich AS and Abel ED. Glucose Metabolism Is Required for Platelet Hyperactivation in a Murine Model of Type 1 Diabetes. *Diabetes*. 2019;68:932-8.
54. Garshick MS, Tawil M, Barrett TJ, Salud-Gnilo CM, Eppler M, Lee A, Scher JU, Neimann AL, Jelic S, Mehta NN, Fisher EA, Krueger JG and Berger JS. Activated Platelets Induce Endothelial Cell Inflammatory Response in Psoriasis via COX-1. *Arterioscler Thromb Vasc Biol*. 2020;40:1340-51.
55. Singethan K and Schneider-Schaulies J. Tetraspanins: Small transmembrane proteins with big impact on membrane microdomain structures. *Commun Integr Biol*. 2008;1:11-3.

56. Wee JL, Schulze KE, Jones EL, Yeung L, Cheng Q, Pereira CF, Costin A, Ramm G, van Spriel AB, Hickey MJ and Wright MD. Tetraspanin CD37 Regulates beta2 Integrin-Mediated Adhesion and Migration in Neutrophils. *J Immunol*. 2015;195:5770-9.
57. Champion TC, Partridge LJ, Ong SM, Malleret B, Wong SC and Monk PN. Monocyte Subsets Have Distinct Patterns of Tetraspanin Expression and Different Capacities to Form Multinucleate Giant Cells. *Front Immunol*. 2018;9:1247.
58. van Spriel AB, de Keijzer S, van der Schaaf A, Gartlan KH, Sofi M, Light A, Linssen PC, Boezeman JB, Zuidscherwoude M, Reinieren-Beeren I, Cambi A, Mackay F, Tarlinton DM, Figdor CG and Wright MD. The tetraspanin CD37 orchestrates the alpha(4)beta(1) integrin-Akt signaling axis and supports long-lived plasma cell survival. *Sci Signal*. 2012;5:ra82.
59. van Spriel AB, Puls KL, Sofi M, Pouniotis D, Hochrein H, Orinska Z, Knobeloch KP, Plebanski M and Wright MD. A regulatory role for CD37 in T cell proliferation. *J Immunol*. 2004;172:2953-61.
60. Gartlan KH, Wee JL, Demaria MC, Nastovska R, Chang TM, Jones EL, Apostolopoulos V, Pietersz GA, Hickey MJ, van Spriel AB and Wright MD. Tetraspanin CD37 contributes to the initiation of cellular immunity by promoting dendritic cell migration. *Eur J Immunol*. 2013;43:1208-19.
61. Sheng KC, van Spriel AB, Gartlan KH, Sofi M, Apostolopoulos V, Ashman L and Wright MD. Tetraspanins CD37 and CD151 differentially regulate Ag presentation and T-cell co-stimulation by DC. *Eur J Immunol*. 2009;39:50-5.
62. de Winde CM, Matthews AL, van Deventer S, van der Schaaf A, Tomlinson ND, Jansen E, Eble JA, Nieswandt B, McGettrick HM, Figdor CG, Tomlinson MG, Acton SE and van Spriel AB. C-type lectin-like receptor 2 (CLEC-2)-dependent dendritic cell migration is controlled by tetraspanin CD37. *J Cell Sci*. 2018;131.
63. Horev MB, Zabary Y, Zarka R, Sorrentino S, Medalia O, Zaritsky A and Geiger B. Differential dynamics of early stages of platelet adhesion and spreading on collagen IV- and fibrinogen-coated surfaces. *F1000Res*. 2020;9.
64. Cohen S, Kamarck T and Mermelstein R. A global measure of perceived stress. *J Health Soc Behav*. 1983;24:385-96.
65. Gau D and Roy P. SRF'ing and SAP'ing - the role of MRTF proteins in cell migration. *J Cell Sci*. 2018;131.
66. Miano JM, Long X and Fujiwara K. Serum response factor: master regulator of the actin cytoskeleton and contractile apparatus. *Am J Physiol Cell Physiol*. 2007;292:C70-81.
67. Nabi H, Kivimaki M, Batty GD, Shipley MJ, Britton A, Brunner EJ, Vahtera J, Lemogne C, Elbaz A and Singh-Manoux A. Increased risk of coronary heart disease among individuals reporting adverse impact of stress on their health: the Whitehall II prospective cohort study. *Eur Heart J*. 2013;34:2697-705.
68. Wang S, Xiaoling G, Pingting L, Shuqiang L and Yuaner Z. Chronic unpredictable mild stress combined with a high-fat diets aggravates atherosclerosis in rats. *Lipids Health Dis*. 2014;13:77.
69. Giannarelli C, Rodriguez DT, Zafar MU, Christoffel D, Vialou V, Pena C, Badimon A, Hodes GF, Mury P, Rabkin J, Alique M, Villa G, Argmann C, Nestler EJ, Russo SJ and Badimon JJ. Susceptibility to chronic social stress increases plaque progression, vulnerability and platelet activation. *Thromb Haemost*. 2017;117:816-8.
70. Lagraauw HM, Wezel A, van der Velden D, Kuiper J and Bot I. Stress-induced mast cell activation contributes to atherosclerotic plaque destabilization. *Sci Rep*. 2019;9:2134.
71. Pekayvaz K, Losert C, Knottenberg V, Gold C, van Blokland IV, Oelen R, Groot HE, Benjamins JW, Brambs S, Kaiser R, Gottschlich A, Hoffmann GV, Eivers L, Martinez-Navarro A, Bruns N, Stiller S, Akgol S, Yue K, Polewka V, Escaig R, Joppich M, Janjic A, Popp O, Kobold S, Petzold T, Zimmer R, Enard W, Saar K, Mertins P, Huebner N, van der Harst P, Franke LH, van der Wijst MGP, Massberg S, Heinig M, Nicolai L and Stark K. Multiomic analyses uncover

immunological signatures in acute and chronic coronary syndromes. *Nat Med*. 2024;30:1696-710.
72. Wang Y, Huang Y, Zhang M, Zhang X, Tang X and Kang Y. Bioinformatic Analysis of the Possible Regulative Network of miR-30a/e in Cardiomyocytes 2 Days Post Myocardial Infarction. *Acta Cardiol Sin*. 2018;34:175-88.
73. Port JD, Walker LA, Polk J, Nunley K, Buttrick PM and Sucharov CC. Temporal expression of miRNAs and mRNAs in a mouse model of myocardial infarction. *Physiol Genomics*. 2011;43:1087-95.
74. Bairey Merz CN, Dwyer J, Nordstrom CK, Walton KG, Salerno JW and Schneider RH. Psychosocial stress and cardiovascular disease: pathophysiological links. *Behav Med*. 2002;27:141-7.
75. Hemler ME. Tetraspanin functions and associated microdomains. *Nat Rev Mol Cell Biol*. 2005;6:801-11.
76. Levy S and Shoham T. The tetraspanin web modulates immune-signalling complexes. *Nat Rev Immunol*. 2005;5:136-48.
77. Boucheix C and Rubinstein E. Tetraspanins. *Cell Mol Life Sci*. 2001;58:1189-205.
78. Lewandrowski U, Wortelkamp S, Lohrig K, Zahedi RP, Wolters DA, Walter U and Sickmann A. Platelet membrane proteomics: a novel repository for functional research. *Blood*. 2009;114:e10-9.
79. Protty MB, Watkins NA, Colombo D, Thomas SG, Heath VL, Herbert JM, Bicknell R, Senis YA, Ashman LK, Berditchevski F, Ouwehand WH, Watson SP and Tomlinson MG. Identification of Tspan9 as a novel platelet tetraspanin and the collagen receptor GPVI as a component of tetraspanin microdomains. *Biochem J*. 2009;417:391-400.
80. Goschnick MW and Jackson DE. Tetraspanins-structural and signalling scaffolds that regulate platelet function. *Mini Rev Med Chem*. 2007;7:1248-54.
81. Uchtmann K, Park ER, Bergsma A, Segula J, Edick MJ and Miranti CK. Homozygous loss of mouse tetraspanin CD82 enhances integrin alphaIIbbeta3 expression and clot retraction in platelets. *Exp Cell Res*. 2015;339:261-9.
82. Goschnick MW, Lau LM, Wee JL, Liu YS, Hogarth PM, Robb LM, Hickey MJ, Wright MD and Jackson DE. Impaired "outside-in" integrin alphaIIbbeta3 signaling and thrombus stability in TSSC6-deficient mice. *Blood*. 2006;108:1911-8.
83. Lau LM, Wee JL, Wright MD, Moseley GW, Hogarth PM, Ashman LK and Jackson DE. The tetraspanin superfamily member CD151 regulates outside-in integrin alphaIIbbeta3 signaling and platelet function. *Blood*. 2004;104:2368-75.
84. Bearer EL, Prakash JM and Li Z. Actin dynamics in platelets. *Int Rev Cytol*. 2002;217:137-82.
85. Bobrowicz M, Kubacz M, Slusarczyk A and Winiarska M. CD37 in B Cell Derived Tumors-More than Just a Docking Point for Monoclonal Antibodies. *Int J Mol Sci*. 2020;21.
86. Hemler ME. Targeting of tetraspanin proteins--potential benefits and strategies. *Nat Rev Drug Discov*. 2008;7:747-58.

Figure 1. Psychosocial Stress Induces Platelet Hyperactivity and Accelerates Thrombosis

(A) Self-reported stress levels in a cohort of cardiovascular disease patients (n = 98). Circulating blood levels of the stable platelet activation markers **(B)** leukocyte-platelet-aggregates (LPA), monocyte-platelet-aggregates (MPA), and neutrophil-platelet-aggregates (NPA) as measured by flow cytometry at the time of stress questionnaire. Grey bars, no stress (n = 60); red bars, several or permanent periods of stress (n = 38). **(C)** Mouse chronic variable stress model. **(D)** Mean platelet volume (MPV), **(E)** reticulated platelets, and **(F)** quantification of LPA, proinflammatory Ly6C^{hi} MPA, and NPA in stress and control mice. White circles, no stress control mice (n = 8); red circles, stressed mice (n = 8). **(G)** Platelet surface expression of the activation markers activated integrin αIIbβ3 and P-selectin following incubation with PBS (Unstim.), epinephrine (10 μM), PAR4-activating peptide (PAR4-AP, 500 μM), or U46619 and ADP (5 μM, receptively) for 15 min. White circles, no stress control mice (n = 7-8); red circles, stressed mice (n = 7-8). **(H-K)** Pulmonary embolism was induced in anesthetized mice by retro-orbital injection of 60 mg/kg epinephrine and 150 mg/kg collagen. **(H)** Time to death was monitored for 45 minutes, and **(I)** Kaplan-Meier survival curve. **(J)** Lung-to-body weight ratio at death and **(K)** pulmonary CD42b staining for platelet aggregates and platelet aggregate quantification. White circles; stress-free control mice (n = 15); red circles, stressed mice (n = 15). Scale bar = 100 μM. Mean ± SEM, *p<0.05, **p<0.01, ***p<0.001 by Student's t-test.

Figure 2. CD37 is Upregulated in Platelets from Stressed Mice and Humans.

Mouse platelet RNA-seq. Platelets were isolated from stress or stress-free control mice at the end of the 3-week chronic variable stress protocol. Platelets were purified, total RNA isolated, and RNA-seq performed. **(A)** Heat map and **(B)** volcano plot of differentially expressed transcripts between stress and control mice (p<0.01). n = 4 samples per group, representing blood from 8 pooled mice per phenotype. Platelets isolated from stressed or stress-free control subjects (Demographics **STable 2**, n = 18 subjects per group). Platelets were purified, total RNA isolated, and RNA-seq performed. **(C)** Heat map and **(D)** volcano plot of differentially expressed transcripts between stressed and stress-free control subjects (p<0.01). **(E)** Spearman's correlation of platelet transcript expression versus platelet aggregation responses to 0.4 μM epinephrine (n = 145 subjects). **(F)** Correlation plots of platelet *CD37* and *SPPL2B* relative to aggregation response to 0.4 μM epinephrine (n = 145 subjects). **(G)** Normalized expression levels of the 22 identified human platelet tetraspanins. CD37 is highlighted in red. **(H)** Correlation matrix of platelet tetraspanins and aggregation responses to epinephrine (Epi; 0.1, 0.4 and 2 μM) and adenosine diphosphate (ADP; 0.1, 0.4 and 2 μM) as measured by light transmission aggregometry. Spearmen correlation, R values displayed in the top panel, p-values in the bottom panel. Correlation of platelet *CD37* expression (x-axis) and the relative eigengene values for pathways **(I)** platelet activation, **(J)** integrin-mediated signaling, **(K)** platelet aggregation and **(L)** regulation of inflammatory responses to wounding (y-axis, n = 183). Associations were assessed by Spearman's rank correlation coefficient.

Figure 3. Absence of CD37 Impairs Platelet Spreading and Activation with no Alterations to Hemostasis

(A) Wild-type and *Cd37*$^{-/-}$ mouse megakaryocyte and platelet *Cd37* expression as determined by RNA-seq. Normalized expression levels are shown. n = 4-6 samples per group. Mean ± SEM, ****p<0.001 by Student's t-test. **(B)** Representative western blot of CD37 and GAPDH of platelets lysates from wild-type and *Cd37*$^{-/-}$ mice. **(C)** Super-resolution microscopy images of platelets immunostained with CD37 (red) and actin filaments (cyan) were reconstructed using the structured illumination microscopy (SIM^2) algorithm. Scale bar = 2 μm. **(D)** Circulating platelet counts, **(E)** prothrombin (PT) and **(F)** partial thromboplastin time (PTT) measured in whole blood (measured by Heska COAG+), and **(G)** time to tail bleeding cessation in wild-type

and *Cd37*$^{-/-}$ mice. Spreading of *Cd37*$^{-/-}$ and wild-type platelets and circularity of adherent platelets assessed by image analysis. Images of cells were assessed by quantification of cell circularity where a value <0.4 equates to a spread/activated platelet (indicated by arrowheads), and >0.7 equates to a minimally spread/activated platelet (indicated by arrows). Platelet spreading on **(H)** poly-D-lysine (50 µg/mL), **(I)** circularity of adherent platelets and the frequency distribution of circularity, categorized as <0.4, 0.4-<0.7, and >0.7, and **(J)** platelet perimeter. Spreading of *Cd37*$^{-/-}$ and wild-type platelets on **(K)** fibrinogen (100 µg/mL), **(L)** circularity of adherent platelets, and the frequency distribution categorized as <0.4, 0.4-<0.7, and >0.7, and **(M)** platelet perimeter. **(N)** Platelet solidity following spreading on fibrinogen (100 µg/mL) for 45 min, and the **(O)** frequency distribution. Grey circles, wild-type mice (n = 4-5); red circles, *Cd37*$^{-/-}$ mice (n = 4-5). At least 5 images and a total of 650 cells were analyzed per mouse. Data are shown as mean ± SEM *p<0.05, **p<0.01, ***p<0.005, ****p<0.0001 as determined by the student's t-test. Scale bar = 10 µm.

Figure 4. CD37 Deficiency Is Protective From Thrombosis

Platelet surface expression of the activation markers **(A)** activated integrin αIIbβ3, **(B)** P-selectin, and **(C)** CD63 following incubation with PBS (no stim) or PAR4-activating peptide (PAR4-AP, 50 µM) for 15 min. Grey circles, wild-type mice (n = 10); red circles, *Cd37*$^{-/-}$ mice (n = 12). $FeCl_3$ carotid thrombosis model in wild-type and *Cd37*$^{-/-}$ mice. **(D)** Mean time to vessel occlusion as measured by a flow probe, **(E)** representative carotid artery blood flow following removal of $FeCl_3$ patch and **(F)** area under the curve (AUC) analysis. Grey circles, wild-type; red circles, *Cd37*$^{-/-}$ mice (n = 10-12 mice per group). Mean ± SEM, *p<0.05, **p<0.05, ****p<0.0001 by Student's t-test.

Figure 5. Platelet CD37 is Increased During Myocardial Infarction and Associates with Stress Levels

(A) Schematic overview of the generation of mature human megakaryocytes from $CD34^+$ stem cells. Megakaryocyte expression of **(B)** activated αIIb/β3 (PAC-1), **(C)** P-selectin and **(D)** CD63 in unstimulated (no stim) or following treatment with thrombin (0.5 U/mL) for 15 minutes (n = 7 unique stem cell donors). Data are shown as a violin plot. P-values were calculated using a paired Student t-test.*P < 0.05; **P < 0.01. Women electively referred for invasive coronary angiography with or without acute coronary syndrome were enrolled in the Heart Attack Research Program (HARP) study. **(E)** MI patients and controls had blood collected for platelet transcriptome and activity measures at the time of coronary angiography. Platelet *CD37* expression in control (n = 38) and MI (n = 40) subjects as determined by RNA-seq, **(F)** stratification of MI subjects into low (PSS-4<6) and high (PSS-4≥6) stress and platelet *CD37* expression. Mean ± SEM, **p<0.01 by Student's t-test. **(G)** Correlation between self-reported stress level and platelet *CD37* expression. **(H)** Platelet *CD37* expression at initial study entry and 3 months post-MI (n = 16 paired samples). **(I)** Overlap of predicted upstream transcriptional regulators as determined by Ingenuity Pathway Analysis of genes differentially expressed in platelets from stressed versus stress-free control subjects or women experiencing a myocardial infarction. ENCODE ChIP-Seq assessment of common CD37 regulators identified to by Ingenuity Pathway Analysis. **(J)** Normalized expression counts of serum response factor (SRF) regulated genes in platelets from stressed versus stress-free control subjects. **(K)** $CD34^+$-derived megakaryocytes were treated with 100 µM aspirin, 5 µM AZD1283 ($P2Y_{12}$ inhibitor), or both aspirin and AZD1283 for 24 hours. **(L)** Megakaryocytes CD37 expression following treatment with anti-platelet therapies or vehicle control. Mean ± SEM, *p<0.05, **p<0.01, ***p<0.005 by Student's t-test.